

**INVESTIGATING THE HISTOMORPHOLOGICAL EFFECT OF *Alstonia*  
*boonei* STEM BARK EXTRACT ON THE LIVER AND KIDNEY OF WISTAR  
ALBINO RATS**

**BY**

**MARTINS MOBOLAJI GLORY**

**BMS 2101503**

**DEPARTMENT OF MEDICAL LABORATORY SCIENCE,  
SCHOOL OF BASIC MEDICAL SCIENCE,  
COLLEGE OF MEDICAL SCIENCES,  
UNIVERSITY OF BENIN,  
BENIN CITY.**

**SEPTEMBER, 2025**

**INVESTIGATING THE HISTOMORPHOLOGICAL EFFECT OF *Alstonia*  
*boonei* STEM BARK EXTRACT ON THE LIVER AND KIDNEY OF WISTAR  
ALBINO RATS**

**BY**

**MARTINS MOBOLAJI GLORY**

**BMS 2101503**

**BEING A PROJECT SUBMITTED TO THE DEPARTMENT OF  
MEDICAL LABORATORY SCIENCE IN PARTIAL FULFILMENT FOR THE  
REQUIREMENT OF THE AWARD OF BACHELORS DEGREE IN MEDICAL  
LABORATORY SCIENCE (BMLS)  
UNIVERSITY OF BENIN, BENIN CITY, NIGERIA.**

**SUPERVISED BY:**

**DR. (MRS). OGEYEMHE**

**SEPTEMBER, 2025.**

## CERTIFICATION

This is to certify that this research work was carried out by **MARTINS MOBOLAJI GLORY** with Matriculation Number **BMS2101503** under the supervision of **DR. (MRS). OGEYEMHE** in the Department of Medical Laboratory Science, University of Benin, Benin City, Edo State.

---

**DR. (MRS). B.E. OGEYEMHE**

(Supervisor)

---

**DATE**

---

**Dr. (MRS). Z. OMORUYI**

(Head of Department)

---

**DATE**

---

**Prof. VICTOR O. EKUNDINA**

(External Examiner)

---

**DATE**

## **DEDICATION**

I dedicate this project work to God Almighty, the giver of knowledge and for His mercy, grace and favour upon my life. To my parents and siblings, their painstaking efforts and sacrifices have brought me this far. To Late **WILLIAMS EFOSA DANIEL** for watching out for me academically and caring for me, continue to Rest in the Bossom of the Lord.

## ACKNOWLEDGEMENTS

My sincere appreciation goes to God Almighty, the giver of knowledge for His love upon my life. My profound appreciation and gratitude also goes to my supervisor **DR. (MRS). B.E OGEYEMHE** for her patience, concern, supportive and constructive idea which aided this project work.

Special appreciation goes to the Head of Department, Medical Laboratory Science, **DR. (MRS). OMORUYI** and to the entire Staff of the department for the support and the various part they played in my academic development. My appreciation goes to **DR. (MRS) P.A OBAZELU** for being a mother and leader to me **and DR. N.T OMORODION** for his role as an academic parent; as well as my Histopathology lecturers, Dr. Mrs. Ehizogie Adeyemi, Dr. E. B. Odigie, Prof Akinbo and Mr Dimowo, their impact cannot be ignored.

My deepest appreciation goes to my Parents (**MR PAUL and MRS LYDIA MARTINS**) and Siblings (**Mr. Banky, Miss. Bukky, Miss. Bolu and Busayomi**) for their love, support, encouragement and prayers in making me come this far in my academic journey. My sincerest appreciation goes to my buddies, **DANNYEL and TAIWO** for their valuable support and contributions, their friendship and support made this journey easier for me. I'm also grateful to my colleagues, HISTOPATHOLOGY '25 and MLS200 for their love and support. God bless you all.

## TABLE OF CONTENTS

|  |      |
|--|------|
| Title Page   | ii   |
| Certification  | iii  |
| Dedication   | iv   |
| Acknowledgements   | v    |
| Table of Contents  | vi   |
| List of Figures  | viii |
| List of Plates   | ix   |
| Abstract   | xvi  |
| <b>CHAPTER ONE: INTRODUCTION</b>   |      |
| 1.1. Background of Study   | 1    |
| 1.2. Statement of Problem  | 2    |
| 1.3. Justification of Study  | 4    |
| 1.4. Significances of Study  | 6    |
| 1.5. Aim of Study  | 8    |
| 1.6. Research Hypothesis   | 8    |
| 1.7. Specific Objectives   | 8    |
| 1.8. Research Questions  | 8    |
| 1.9. Study Limitation  | 9    |
| <b>CHAPTER TWO: LITERATURE REVIEW</b>                                    |      |
| 2.1. <i>Alstonia boonei</i>  | 11   |
| 2.2. <i>Alstonia boonei</i> : Botanical Description and Traditional Uses | 12   |
| 2.3. Nutritional and Ethnomedicinal uses of <i>Alstonia boonei</i>       | 16   |
| 2.4 Phytochemical constituents of <i>Alstonia boonei</i>                 | 17   |
| 2.5 Pharmacological activities of <i>Alstonia boonei</i>                 | 19   |
| 2.5.1 Hepatoprotective activity of <i>Alstonia boonei</i>                | 20   |
| 2.5.2 Nephroprotective activity of <i>Alstonia boonei</i>                | 21   |
| <b>CHAPTER THREE: MATERIALS AND METHODS</b>                              |      |
| 3.1 Materials, Reagents and Equipments for Research                      | 30   |

|                              |  |        |
|------------------------------|--|--------|
| 3.1.1                        | Materials  | 30     |
| 3.1.2                        | Reagents Used  | 30     |
| 3.1.3                        | Equipment Used   | 30     |
| 3.1.4                        | Reagents and Chemicals   |        |
|                              | 31   |        |
| 3.2                          | Collection of Experimental Plant Materials   |        |
|                              | 31   |        |
| 3.2.1                        | Identification and Authentication  | 31     |
| 3.2.2                        | Preparation of Plant Material  |        |
|                              | 31   |        |
| 3.3                          | Animal Housing   |        |
|                              | 32   |        |
| 3.4                          | Ethical Approvals  |        |
|                              | 32   |        |
| 3.5                          | Methodology  |        |
|                              | 33   |        |
| 3.5.1                        | Experimental   | Design |
|                              | 33   |        |
| 3.5.2                        | Experimental grouping and dosage administration of <i>Alstonia boonei</i> stem bark extract on rats. | 34     |
| 3.5.3                        | Dosage Calculations  | 35     |
| 3.6                          | Histopathological studies  | 35     |
| 3.6.1                        | Histological Technique   | 36     |
| 3.7                          | Microscopy and Photomicrography  | 39     |
| 3.7.1                        | Statistical Analysis   |        |
|                              | 39   |        |
| <b>CHAPTER FOUR: RESULTS</b> |  |        |
| 4.1                          | Histopathological Examination  | 40     |
| 4.7                          | Statistics Analysis  | 59     |

|                                 |           |
|---------------------------------|-----------|
| <b>CHAPTER FIVE: DISCUSSION</b> | <b>63</b> |
| 5.1 Discussion of Findings      | 63        |
| 5.2 Recommendations             | 64        |
| <b>REFERENCES</b>               | <b>65</b> |
| <b>APPENDIX</b>                 | <b>69</b> |

## LIST OF FIGURES

|  |    |
|--|----|
| Figure 2.1 Stem and Leaf of <i>Alstonia boonei</i> | 15 |
| Figure 2.2 Anatomy of the Liver                    | 24 |
| Figure 2.3 Anatomy of the kidneys                  | 27 |

## LIST OF PLATES

**Plate 4.1A:** Section of the liver from the control rats showed hepatocytes (arrow) with eosinophilic cytoplasm surrounding a centrally placed normochromic nucleus with indistinct nucleoli. The hepatocytes were arranged in cords separated by clear, non-congested sinusoids. **FEATURES IN KEEPING WITH NORMAL HEPATOCYTES. H and E. Mag x400**

**Plate 4.1B:**Section of the liver from the control rat showed hepatocytes (arrow) with abundant eosinophilic cytoplasm arranged in radial cords around patent hepatic sinusoids. Each cell contained a centrally placed normochromic nucleus with indistinct nucleoli, and no visible signs of inflammation, necrosis, or congestion were observed. **FEATURES IN KEEPING WITH NORMAL HEPATOCYTES. H and E. Mag x400**

**Plate 4.1C:** Section of the kidney from control rats showed intact glomeruli (left arrow) with well-preserved Bowman's capsule and renal tubules (right arrow) lined by cuboidal epithelium with distinct nuclei. **FEATURES IN KEEPING WITH NORMAL RENAL HISTOLOGY. H and E. Mag x400.**

**Plate 4.1D:** Section of the kidney from the control group showed intact glomeruli (large arrow) with well-defined capillary loops and normal Bowman's space. The renal tubules (small arrow) displayed cuboidal epithelium with clear cytoplasm and centrally placed nuclei. **FEATURES IN KEEPING WITH NORMAL RENAL HISTOARCHITECTURE. H and E. Mag x400.**

**Plate 4.2A:** Section of the liver from rats administered low-dose *Alstonia boonei* stem bark extract showed mildly swollen hepatocytes with granular eosinophilic cytoplasm and prominent, centrally placed nuclei. Mild sinusoidal dilation was observed with otherwise preserved hepatic architecture. **FEATURES SUGGESTIVE OF MILD HEPATOCELLULAR REACTIVE CHANGES. H and E. Mag x400**

**Plate 4.2B:** Section of the liver from rats administered low-dose *Alstonia boonei* stem bark extract showed preserved hepatic architecture with hepatocytes (arrow) exhibiting mildly eosinophilic cytoplasm and centrally placed normochromic nuclei. Sinusoids appeared slightly dilated, and mild cytoplasmic swelling was observed in some hepatocytes. **FEATURES SUGGESTIVE OF MILD HEPATOCELLULAR REACTIVE CHANGES. H and E. Mag x400**

**Plate 4.2C:** Section of the kidney from rats in group B showed intact glomeruli (large arrow) with normal cellularity and patent Bowman's space. The surrounding renal tubules (small arrow) exhibited normal cuboidal epithelium with preserved brush borders. **FEATURES IN KEEPING WITH NORMAL RENAL HISTOLOGY. H and E. Mag x400.**

**Plate 4.2D:** Section of the kidney shows normal glomerulus (large arrow) with intact capillary loops and well-defined Bowman's space. The surrounding renal tubules (small arrow) exhibit preserved epithelial lining with no evident cellular degeneration or necrosis. **FEATURES IN KEEPING WITH NORMAL RENAL HISTOLOGY. H and E. Mag x400.**

**Plate 4.3A:** Section of the liver from rats administered a higher dose of *Alstonia boonei* stem bark extract showed dilated hepatic sinusoids and hepatocytes (arrow) with vacuolated eosinophilic cytoplasm, some appearing mildly distorted. The nuclei were centrally placed but showed occasional chromatin condensation. **FEATURES IN KEEPING WITH MODERATE HEPATOCELLULAR DEGENERATION. H and E. Mag x400.**

**Plate 4.3B:** Section of the liver from rats administered higher-dose *Alstonia boonei* stem bark extract revealed dilated sinusoids, hepatocytes with vacuolated cytoplasm, and distortion of hepatic cords. Nuclei were still visible but slightly irregular in shape, with scattered chromatin condensation. **FEATURES IN KEEPING WITH MODERATE TUBULAR DEGENERATION. H and E. Mag x400.**

**Plate 4.3C:** Section of the kidney from rats in group C showed well-defined glomeruli (large arrow) with normal cellularity and intact Bowman's space. The adjacent renal tubules (small arrow) exhibited preserved epithelial lining with no signs of degeneration or necrosis. **FEATURES CONSISTENT WITH NORMAL RENAL HISTOLOGY. H and E. Mag x400.**

**Plate 4.3D:** Section of the kidney from rats in group C showed normal renal corpuscles (large arrow) with intact glomerular tufts and well-defined Bowman's capsules. The surrounding renal tubules (small arrow) exhibited preserved epithelial lining with no evidence of tubular degeneration or necrosis. **FEATURES**

**CONSISTENT WITH NORMAL RENAL HISTOLOGY. H and E. Mag x400.**

**Plate 4.4A:** Section of the liver showed hepatocytes (arrow) with eosinophilic cytoplasm, some appearing vacuolated and slightly disorganized. The hepatic cords appear narrowed, with dilated sinusoids and occasional pyknotic nuclei visible. No widespread necrosis is seen, but there is evidence of mild to moderate hepatocellular degeneration.

**FEATURES SUGGESTIVE OF MODERATE HEPATOCELLULAR REACTIVE CHANGES WITH EARLY DEGENERATIVE FEATURES. H and E. Mag x400**

**Plate 4.4B:** Section of the liver from rats administered 400 mg/kg of *Alstonia boonei* stem bark extract showed moderate distortion of hepatic architecture, with hepatocytes (arrow) exhibiting cytoplasmic vacuolation and loss of cellular boundaries. The nuclei appeared mildly hyperchromatic, with areas showing sinusoidal dilatation and moderate hepatocellular degeneration.

**FEATURES IN KEEPING WITH MODERATE DEGENERATIVE CHANGES. H and E. Mag x400**

**Plate 4.4C:** The kidney section from group D shows glomeruli (large arrow) with slight congestion and mild enlargement, but overall preserved architecture. The surrounding renal tubules (small arrow) appear mostly intact with minimal tubular epithelial cell swelling. There is mild interstitial inflammation indicated by scattered

inflammatory cells (small arrow at the upper left). **FEATURES SUGGEST MILD RENAL TISSUE RESPONSE POSSIBLY DUE TO TREATMENT OR EARLY**

**SIGNS OF RENAL STRESS. H & E. Mag x400.**

**Plate 4.4D:** Section of the kidney from Rat B, group D, administered 400mg/kg of *Alstonia boonei* stem bark, shows glomerulus (arrow) with normal cellularity and surrounding renal tubules (arrow) with preserved architecture. There is mild vascular congestion in the interstitium. **FEATURES IN KEEPING WITH MINIMAL TO NO PATHOLOGIC CHANGES. H and E. Mag x400.**

**Plate 4.5A:** Section of the liver from rat administered 600 mg/kg of *Alstonia boonei* stem bark shows hepatocytes (arrow) with mildly eosinophilic cytoplasm and centrally placed normochromic nuclei. Hepatic cords appear preserved, with slightly dilated sinusoids. No significant necrosis, inflammation, or cellular degeneration is observed. **FEATURES IN KEEPING WITH MILDLY ALTERED BUT PRESERVED HEPATIC ARCHITECTURE. H&E stain. Mag. x400.**

**Plate 4.5B:** Section of the liver from rats administered 800 mg/kg of *Alstonia boonei* stem bark extract revealed distorted hepatic architecture with marked hepatocellular degeneration. Hepatocytes (arrow) showed cytoplasmic vacuolation, eccentric and hyperchromatic nuclei, and loss of cell-to-cell boundaries. There is mild sinusoidal dilatation and congestion, indicating toxic hepatocellular injury. **FEATURES IN KEEPING WITH SEVERE DEGENERATIVE CHANGES. H and E. Mag x400.**

**Plate 4.5C:** Section of the kidney from Rat A showed a renal corpuscle (arrow) with mildly hypercellular glomeruli and focal mesangial prominence. The surrounding tubules (arrow) revealed patchy epithelial degeneration with widened tubular lumens

and interstitial infiltration by inflammatory cells. **FEATURES SUGGESTIVE OF**

**MODERATE GLOMERULAR AND TUBULAR INJURY. H and E. Mag x400**

**Plate 4.5D:** Section of the kidney from Rat B showed a mildly hypercellular glomerulus (arrow) with preserved architecture. The surrounding renal tubules (arrow) appeared mostly intact, though with occasional tubular dilation and sparse interstitial spaces. **FEATURES SUGGESTIVE OF MILD RENAL STRESS WITH RELATIVELY PRESERVED STRUCTURE. H and E. Mag x400.**

**Plate 4.6A:** Section of the liver from rat administered 800 mg/kg of *Alstonia boonei* stem bark shows hepatocytes (arrow) with eosinophilic cytoplasm and mildly pleomorphic nuclei. There is evidence of sinusoidal dilatation and mild disruption in hepatic cord arrangement. However, no overt necrosis or inflammatory infiltrate is observed. **FEATURES IN KEEPING WITH MILD HEPATOCELLULAR ALTERATION AND SINUSOIDAL DILATATION. H&E stain. Mag. x400.**

**Plate 4.6B:** Section of the liver from Rat B group F (administered 800mg/kg of *Alstonia boonei* stem bark) showed hepatocytes (arrow) with mildly eosinophilic cytoplasm and some areas of cellular distortion with slight infiltration of inflammatory cells. **FEATURES SUGGESTIVE OF MILD HEPATOCYTE INJURY. H and E. Mag x400.**

**Plate 4.6C:** Section of the kidney from Rat A showed distorted renal architecture with a glomerulus (arrow) exhibiting marked hypercellularity and congestion. The surrounding renal tubules (arrow) appeared dilated with flattened epithelial lining and

extensive interstitial spaces. **FEATURES INDICATIVE OF SEVERE**

**GLOMERULAR AND TUBULAR DAMAGE. H and E. Mag x400**

**Plate 4.6D:** Section of the kidney from Rat B revealed a severely altered glomerulus (arrow) with loss of structural detail and marked cellular infiltration. Tubular structures (arrow) showed widespread epithelial degeneration, vacuolization, and interstitial edema. **FEATURES IN KEEPING WITH ADVANCED NEPHROTOXIC DAMAGE. H and E. Mag x400.**

## ABSTRACT

*Alstonia boonei*, a plant species known for its medicinal properties and a tropical tree native to Africa, may exhibit protective effects on some vital organs. Various parts of the tree, including the bark, leaves, and roots, have been used in traditional medicine for their anti-inflammatory, antimicrobial, and antioxidant properties. The aim of this study is to evaluate the histomorphological effects of *Alstonia boonei* stem bark extract on the liver and kidney of Wistar albino rats. Thirty healthy rats were separated into groups and housed in controlled conditions. Histopathological examinations will assess potential damage or protective effects. Given *Alstonia boonei*'s potential antioxidant and anti-inflammatory properties, it may offer benefits for liver and kidney health. The results of this study may provide insights into the potential therapeutic applications of *Alstonia boonei* in preventing liver and kidney damage. Some studies suggest that *Alstonia boonei* stem bark extract may have hepatoprotective properties, reducing liver damage and inflammation. Additionally, it may alleviate hyperlipidemia and renal malfunctions in benign prostatic hyperplasia-induced rats . Further research is needed to explore the mechanisms underlying these effects and to determine the optimal dosage for maximum protection.

## CHAPTER ONE

### INTRODUCTION

#### 1.1. Background of Study

Over the past few decades, scientific interest in herbal medicine has significantly intensified, revealing the therapeutic value of numerous indigenous plant species, particularly within tropical and subtropical zones where traditional healing practices continue to play a central role in primary healthcare delivery (Olanlokun and Olorunsogo, 2018). Among these medicinal plants, *Alstonia boonei*, a perennial evergreen belonging to the Apocynaceae family, has received increasing scholarly attention due to its broad pharmacological applications that span antimalarial, anti-inflammatory, analgesic, and antidiabetic purposes (Adjouzem et al., 2020; Akintunde et al., 2016). In several countries across sub-Saharan Africa, *A. boonei* remains a widely utilized component of ethnomedicine, especially for managing persistent health problems such as liver and kidney disorders, chronic inflammatory conditions, and fever-related illnesses (Mbiantcha et al., 2020). The stem bark of this species holds particularly high medicinal value because it contains a rich spectrum of phytochemicals, including alkaloids, flavonoids, saponins, tannins, and polyphenols, each of which is recognized for contributing to its therapeutic efficacy (Nwaehujor et al., 2019).

The liver and kidneys are vital organs that play critical roles in detoxification, metabolism, and homeostasis (Guyton & Hall, 2016). Any compromise of these organs' structure or function can lead to systemic toxicity, metabolic disorders, and disease progression (Guyton & Hall, 2016). Given the potential impact of herbal extracts on liver and

kidney function, it is essential to evaluate the histological architecture of these organs after administration of plant-based extracts such as that of *A. boonei*. Despite its longstanding traditional usage, rigorous scientific evaluations aimed at confirming its safety, especially concerning potential microscopic or histopathological impacts on vital tissues like the liver and kidneys, remain limited and in some cases inconclusive (Gandhi et al., 2023).

The liver is an essential biological interface, responsible for metabolizing nutrients and detoxifying harmful substances (Jeganathan et al., 2024). Any compromise of this protective structure whether due to oxidative injury or chemical insult can impair liver function, destabilize homeostasis, and trigger systemic inflammation, thereby accelerating disease progression (Jeganathan et al., 2024). Similarly, the kidneys play a crucial role in maintaining electrolyte balance and regulating blood pressure (Guyton & Hall, 2016). Given these concerns, assessing the histological architecture of liver and kidney tissues after administration of plant-based extracts such as that of *A. boonei* becomes critically important for establishing both efficacy and safety.

Past toxicological studies have produced mixed findings, with differences in reported outcomes often linked to factors such as extraction solvent, administered dosage, and duration of exposure (Olanlokun and Olorunsogo, 2018). For instance, both methanolic and aqueous stem bark extracts of *A. boonei* have demonstrated the ability to reduce oxidative stress and promote tissue recovery in experimental models of liver and kidney damage (Adjouzem et al., 2020; Gandhi et al., 2023). Conversely, prolonged administration at high doses has been associated with mild to moderate histopathological alterations, including vacuolation, degeneration, and focal tissue damage within both liver and kidney structures (Olanlokun and Olorunsogo, 2018).

A growing body of experimental research also highlights the plant's modulatory influence on oxidative stress markers and immune-inflammatory mediators within the liver and kidneys (Akintunde et al., 2016). For example, Akintunde et al. (2016) reported that *A. boonei* stem bark extract mitigated oxidative damage and inflammation in liver and kidney tissues of diabetic rat models by regulating pro-inflammatory enzymes such as cyclooxygenase-2 (COX-2) and inducible nitric oxide synthase (iNOS). Similarly, Adjouzem et al. (2020) found that treatment with *A. boonei* significantly alleviated both macroscopic and microscopic manifestations of liver and kidney damage in experimental models, suggesting a promising role for the plant as a natural therapeutic agent.

Against this background, the present study seeks to determine whether stem bark extract of *A. boonei* exerts a protective influence on liver and kidney histology or induces any notable histopathological alterations when examined through light microscopy, thereby contributing to evidence-based assessments of its safety and medicinal relevance (Mbiantcha et al., 2020; Nwaehujor et al., 2019).

## **1.2 Statement of the Problem**

Despite the frequent application of *Alstonia boonei* in indigenous medical practices for treating a variety of liver and kidney disorders, there remains a substantial lack of empirical evidence addressing its precise histological impacts on mammalian liver and kidney tissues (Olanlokun and Olorunsogo, 2018; Adjouzem et al., 2020). Although the stem bark extract of this plant is often commended for possessing anti-inflammatory and antioxidant activities, such pharmacological claims are not yet consistently substantiated by extensive microscopic and toxicological

investigations (Ojo et al., 2014; Akintunde et al., 2016).

Furthermore, certain bioactive constituents found in *A. boonei*, including alkaloids and tannins, while advantageous at controlled dosages, have been linked to cytotoxic and potentially mutagenic outcomes when administered in excessive quantities or over prolonged durations (Mbiantcha et al., 2020). This raises legitimate concerns regarding the possibility of structural impairment to key liver and kidney components, particularly under conditions of chronic use (Awodele et al., 2010; Adjouzem et al., 2020). Experimental evidence from animal studies further reveals that liver and kidney responses to plant-derived extracts may vary considerably, with outcomes influenced by variables such as the dosage level, extraction technique, and exposure period (Oshomoh and Imoyera, 2019; Akinmurele et al., 2023). Consequently, the absence of comprehensive histological evaluation of the liver and kidney effects of *A. boonei* stem bark extract, especially within controlled experimental models such as Wistar albino rats, emphasizes an urgent need for focused investigation (Adjouzem et al., 2020; Omitola, 2021). Considering the plant's extensive utilization in traditional healing systems, it becomes imperative to establish whether its administration confers protective benefits or induces morphological damage to the liver and kidneys (Adjouzem et al., 2020; Omitola, 2021). This study aims to address this knowledge gap and provide evidence-based assessments of the safety and medicinal relevance of *A. boonei*.

### **1.3 Justification of the Study**

Medicinal plants, including *Alstonia boonei*, are experiencing a surge in global acceptance (Olanlokun and Olorunsogo, 2018), particularly within African communities where indigenous healing traditions remain a central pillar of healthcare delivery (Uroko et al., 2020). Despite this

growing reliance, comprehensive preclinical evaluations especially those targeting vital organs such as the liver and kidneys are still insufficient. As the popularity of plant-based therapies continues to escalate, there is a pressing need for scientific validation of both their beneficial effects and possible adverse outcomes (Akinmurele et al., 2023), with emphasis on experimental models that accurately reflect human physiological mechanisms (Uroko et al., 2020).

The stem bark of *A. boonei* contains a spectrum of bioactive molecules such as alkaloids, tannins, and flavonoids (Mbiantcha et al., 2020), which may confer therapeutic value but also have the potential to produce toxic effects depending on concentration and duration of exposure (Uroko et al., 2020; Akinmurele et al., 2023). The current investigation is driven by the need to determine whether prolonged ingestion of *A. boonei* stem bark extract leads to improvement or deterioration of the liver and kidney histology under controlled experimental conditions (Mbiantcha et al., 2020). The liver and kidneys are essential organs that play critical roles in detoxification, metabolism, and homeostasis (Guyton & Hall, 2016). Any compromise of these organs' structure or function can lead to systemic toxicity, metabolic disorders, and disease progression (Guyton & Hall, 2016). By employing Wistar albino rats recognized as reliable analogues for human liver and kidney physiology, this study seeks to clarify the plant's role in maintaining or altering liver and kidney structural integrity (Ileke et al., 2014; Omitola, 2021).

The findings of this research are expected to contribute to safer and more informed use of *A. boonei* in complementary medicine and provide valuable reference points for public health authorities and regulatory bodies concerned with the toxicological safety of herbal products (Ajadi et al., 2022). Furthermore, this study will help to establish a scientific basis for the traditional use of *A. boonei* and provide insights into its potential therapeutic applications (Adjouzem et al., 2020).

In conclusion, this study is justified by the need for scientific validation of the safety and efficacy of *A. boonei* stem bark extract, particularly in relation to its potential impact on liver and kidney histology. The study's findings will contribute to the growing body of evidence on the therapeutic potential of medicinal plants and inform the development of safe and effective herbal remedies.

#### **1.4 Significance of the Study**

Investigating the histopathological impact of *Alstonia boonei* stem bark extract on the kidney and liver of Wistar albino rats is essential for two primary purposes: safeguarding public health and advancing evidence-based applications of herbal medicine (Nkono et al., 2015; Oyebode, 2018). This necessity arises because the increasing global and African dependence on traditional medicinal remedies demands scientific validation supported by thorough toxicological and microscopic analyses (Nkono et al., 2015; Oyebode, 2018).

Histological examination serves as a dependable tool for identifying alterations at the tissue level (Oshomoh and Imoyera, 2019), enabling researchers to accurately determine cell viability, inflammatory responses, and modifications in kidney and liver structures following exposure to plant-derived extracts or pharmacological agents (Oshomoh and Imoyera, 2019). The kidney and liver are particularly significant in this context because they are vital organs that play critical roles in detoxification, metabolism, and homeostasis (Guyton & Hall, 2016).

Structural damage to these tissues can cause serious consequences such as impaired organ function, persistent inflammation, and potentially systemic toxic effects (Guyton & Hall, 2016). Earlier investigations on *A. boonei* extracts both aqueous and methanolic have revealed dual outcomes, demonstrating beneficial as well as harmful effects depending on the dosage administered and the

length of treatment (Adjouzem et al., 2020).

The present study is crucial in determining the therapeutic window for *A. boonei*, that is, the dosage range where positive outcomes are optimized and harmful effects are minimized (Adotey et al., 2012; Oyeboode, 2018). Such findings are vital for informing public health guidelines, improving the formulation of herbal products, and aiding standardization protocols within traditional medical practice (Oyeboode, 2018).

Additionally, these results contribute to the responsible progression of novel plant-based therapeutic agents that are both clinically effective and safe for human use (Adotey et al., 2012; Oyeboode, 2018), thereby promoting scientifically grounded practices in ethnomedicine (Oyeboode, 2018). Furthermore, this research generates fundamental preclinical data that can support subsequent clinical investigations and potentially facilitate the integration of *A. boonei* into national and global pharmacopeias (Awodele et al., 2010).

It also addresses a significant knowledge gap regarding the kidney and liver safety profile of traditional herbal remedies, while supplying policymakers and regulatory agencies with the scientific basis necessary to establish safety standards for herbal products that are extensively consumed worldwide (Awodele et al., 2010). The study's findings will have implications for the safe use of *A. boonei* in traditional medicine

and will contribute to the growing body of evidence on the therapeutic potential of medicinal plants.

## **1.5 Aim of the Study**

This study aimed at investigating the histopathological effects of *Alstonia boonei* stem bark extract on the liver and kidneys of Albino rats.

## **1.6 Research Hypothesis**

Ha1: The administration of *Alstonia boonei* stem bark extract produces a dose-related alteration in the structural features of the liver and kidneys in albino rats.

Ha2: The administration of *Alstonia boonei* stem bark extract produces a dose-related alteration in the overall histological characteristics of the liver and kidneys in albino rats.

## **1.7 Specific Objectives of the Study**

This research aimed to:

1. Assess how *Alstonia boonei* stem bark extract influences the histopathology of the liver and kidney tissues in albino rats.
2. Determine the influence of *Alstonia boonei* stem bark extract on biochemical markers that indicate liver and kidney function in albino rats.

## **1.8 Research Questions**

### **1.8.1 Null Hypotheses (H):**

1. There is no significant histomorphological change in the liver and kidney tissues of

Wistar rats treated with *Alstonia boonei* stem bark extract compared to control rats.

2. There is no significant alteration in biochemical parameters related to liver and kidney function

in Wistar rats treated with *Alstonia boonei* stem bark extract compared to control rats.

### **1.8.2 Alternative Hypotheses (H):**

1. To what extent does *Alstonia boonei* stem bark extract modify the histopathology of the liver and kidneys in albino rats?

2. To what extent does *Alstonia boonei* stem bark extract alter liver and kidney function–related biomarkers in albino rats?

### **1.9. Study Limitation**

**Use of animal models:** This study uses Wistar albino rats as animal models, which may not accurately represent the human population. The results of this study may not be directly applicable to humans. They are prone to certain diseases for example infections and some types of tumors. It means that the studied population may have higher sensitivity to disease and its manifestations, which may influence the results of studies, when disease processes or potential treatments are examined. The other limitation is that Albino Wistar rat has a relatively shorter life span than any other

strain of rats. Reduced life expectancy can also reduce the possibilities of research, especially in trials concerned with aging or late outcomes of interventions (Krubaa, 2024)

**Limited sample size:** The sample size of this study is limited, which may not provide sufficient statistical power to detect significant differences between treatment groups. A larger sample size may be required to confirm the findings of this study.

**Short duration of study:** The duration of this study is limited, which may not allow for the full

manifestation of the Histomorphological effects of *Alstonia boonei* stem bark extract on the liver and kidney. A longer duration of study may be required to fully investigate the effects of *Alstonia boonei* stem bark extract.

**Lack of mechanistic studies:** This study does not investigate the mechanisms by which *Alstonia boonei* stem bark extract affect the morphology of tissues and influence liver and kidney function–related biomarkers in albino rats. Further studies are required to elucidate the mechanisms of action of *Alstonia boonei* stem bark extract.

**Limited generalizability:** The results of this study may not be generalizable to other populations, such as humans with underlying medical conditions or those taking other medications. Further studies are required to investigate the histomorphological effects of *Alstonia boonei* stem bark extract in different populations

## CHAPTER TWO

### LITERATURE REVIEW

#### 2.1 *Alstonia boonei*

For centuries, medicinal plants have served as the foundation of healthcare systems in numerous African communities (Adotey et al., 2012), with *Alstonia boonei* ranking among the most widely relied-upon species due to its extensive range of ethnomedicinal applications (Adotey et al., 2012). This evergreen tree is indigenous to the tropical rainforest zones of West Africa (Adotey et al., 2012) and is popularly referred to by local populations as the “God’s Tree” because of its revered status in traditional healing systems (Adotey et al., 2012).

In folk medicine, it is frequently employed for addressing illnesses such as malaria, fever, rheumatic conditions, and a variety of liver and kidney disorders (Adotey et al., 2012). The stem bark, in particular, is often processed into an oral decoction to alleviate liver and kidney discomfort (Okorie et al., 2022). With the growing global interest in plant-based therapeutic remedies (Nkono et al., 2015), there is a pressing need to validate such traditional practices through robust experimental and clinical evidence (Nkono et al., 2015).

Phytochemical investigations have revealed that extracts from *A. boonei* contain diverse bioactive compounds, including alkaloids, flavonoids, tannins, and triterpenoids (Akinmurele et al., 2023), each associated with antimicrobial, anti-inflammatory, and antioxidant effects (Nkono et al., 2015).

However, when

consumed in excessive doses or prepared incorrectly, these same compounds can pose toxicity risks, particularly to the liver and kidneys, which are critical organs involved in detoxification and

metabolism (Anyanwu et al., 2020).

Maintaining the structural and functional integrity of the liver and kidneys is critical for effective metabolism, immune system regulation, and protection against pathogenic invasion (Akintunde et al., 2016). Disruption of these organs can result in metabolic disorders, chronic inflammation, or systemic toxicity (Akintunde et al., 2016). Consequently, examining the histopathological impact of herbal preparations like *A. boonei* is essential to establishing accurate safety profiles (Akintunde et al., 2016). Emerging experimental data suggest that *A. boonei* may exert both beneficial and harmful influences on liver and kidney tissues (Okorie et al., 2022), depending on variables such as concentration, extraction technique, and treatment duration (Nkono et al., 2015). Given its widespread, and often unregulated, application in traditional medicine (Adjouzem et al., 2020), there is a significant need for empirical studies to bridge the knowledge gap between ancestral practices and modern biomedical understanding (Adjouzem et al., 2020).

This research therefore seeks to evaluate the histological outcomes of *A. boonei* stem bark extract on the liver and kidney tissue of Wistar albino rats (Adjouzem et al., 2020), with the aim of delivering evidence-based insights to inform safe herbal use, guide policy regulation, and contribute to the scientific discourse surrounding plant-derived medicinal agents (Adjouzem et al., 2020).

## **2.2 *Alstonia boonei*: Botanical Description and Traditional Uses**

*Alstonia boonei* De Wild is a tall, deciduous species belonging to the Apocynaceae family (Ngbolua et al., 2022), thriving predominantly in humid, tropical forest environments across West and Central Africa (Ngbolua et al., 2022). Mature specimens can grow to heights of up to 45

meters (Ngbolua et al., 2022), typically exhibiting a straight trunk covered in gray bark that exudes a sticky, milky latex when cut (Ngbolua et al., 2022). The foliage consists of simple, glossy, oblong leaves arranged in whorls of three to ten along the stem (Oluyori et al., 2020). The reproductive structures include small, greenish-white flowers borne in clustered inflorescences, which develop into elongated follicles containing numerous seeds equipped with silky hairs to aid wind dispersal (Oluyori et al., 2020). Geographically, *A. boonei* is native to multiple African countries, including Nigeria, Ghana, Cameroon, and regions of the Democratic Republic of Congo (Betti et al., 2015; WafoBorel et al., 2022). Its adaptability to varied soil conditions and climates has contributed to its broad distribution (Wafo Borel et al., 2022), as has its enduring cultural and medicinal relevance (Ngbolua et al., 2022). The species is venerated in many traditional societies, known as “Onyame dua” or “God’s Tree” in Ghana and “Egbu” in southeastern Nigeria (Ngbolua et al., 2022). The stem bark remains the most intensively harvested component (Opoku andl Akoto, 2015), commonly boiled into a decoction to address ailments such as malaria, hypertension, arthritis, stomach ulcers, and general digestive disturbances (Opoku andl Akoto, 2015)

Rich in tannins, it is also applied in treating wounds and microbial infections (Opoku andl Akoto, 2015). Beyond medicine, the plant features prominently in spiritual rituals and cultural ceremonies, often serving both healing and symbolic roles (Ngbolua et al., 2022). From an ecological and economic perspective, *A. boonei* offers multiple benefits (Betti andl Ambara, 2014). Its timber, prized for being lightweight yet durable, is used in furniture and construction (Betti andl Ambara, 2014), while the bark serves as a key raw material in commercial herbal formulations (Betti andl Ambara, 2014). Nonetheless, escalating demand has raised sustainability concerns

(Betti andl Ambara, 2014), prompting calls for regulated harvesting and studies on the species' regeneration capacity (Betti andl Ambara, 20).



**Figure 2.1 Stem and Leaf of *Alstonia boonei* (Ngbolua et al., 2022).**

### **2.3. Nutritional and Ethnomedicinal Uses of *Alstonia boonei***

*Alstonia boonei* De Wild., a large perennial tree widely distributed in the tropical forests of West and Central Africa, is highly valued for both its nutritional constituents and broad ethnomedicinal significance (Burkill, 1985). Different parts of the plant—including the bark, leaves, root, and latex have been studied for their bioactive compounds and therapeutic potential. Phytochemical investigations reveal that *A. boonei* contains alkaloids, tannins, flavonoids, saponins, and phenolic compounds that contribute to its pharmacological activities (Akinmoladun et al., 2018). Nutritionally, the leaves and bark are reported to contain minerals such as calcium, iron, magnesium, and potassium, along with modest amounts of proteins and carbohydrates, which support their use as fortifying herbal supplements in local diets (Ezekwesili et al., 2010). The bark of *A. boonei* is particularly renowned for its antipyretic, analgesic, and anti-inflammatory properties, making it a widely used herbal remedy for fever, malaria, and rheumatic pain in African ethnomedicine (Iwu, 2014). Decoctions and infusions prepared from the stem bark are commonly administered for malaria, headaches, and general body weakness (Olajide et al., 2000). The leaves are employed in poultices for treating skin infections, wounds, and ulcers, while the latex is used externally for toothache, sores, and local anesthetic purposes (Akinmoladun et al., 2018). Root extracts are used in managing gastrointestinal disorders such as diarrhea, dysentery, and stomachache, reflecting the plant's broad therapeutic application (Burkill, 1985).

Beyond human medicine, *A. boonei* has ethnoveterinary applications. Livestock

herders utilize bark and leaf extracts to treat parasitic infections, wounds, and fever in animals, demonstrating its multipurpose role in traditional veterinary practices (Nworu et al., 2010). In

some communities, the powdered bark is also administered as an anthelmintic, helping to expel intestinal worms in both humans and animals. The widespread usage of the plant across diverse regions underscores its status as a “therapeutic tree,” comparable to other widely utilized medicinal species in tropical Africa (Iwu, 2014).

Pharmacological studies corroborate many of these traditional claims. Extracts of *A. boonei* have demonstrated significant antimalarial, anti-inflammatory, antioxidant, antimicrobial, and analgesic activities in experimental models (Olajide et al., 2000; Akinmoladun et al., 2018). The alkaloid fraction, particularly echitamine, has attracted research attention for its anticancer potential, while the bark’s bitter principle is linked to antimalarial efficacy (Akinmoladun et al., 2018). However, as with many medicinal plants, concerns regarding dosage, safety, and standardization persist. Excessive consumption of concentrated extracts may cause adverse effects, and variations in preparation methods contribute to inconsistent outcomes (Ezekwesili et al., 2010).

*Alstonia boonei* represents a nutritionally modest but pharmacologically rich plant resource with wide-ranging ethnomedicinal applications. Its use in treating malaria, fever, inflammation, pain, and gastrointestinal disorders has been validated by both traditional practice and modern pharmacological research. The continued study and standardization of its bioactive components could provide safer and more effective

therapeutic agents, while preserving its cultural and ecological importance in African traditional medicine.

#### **2.4 Phytochemical Constituents of *Alstonia boonei***

*Alstonia boonei* is widely acknowledged as an important medicinal species across West Africa,

where it has been traditionally applied for centuries to treat numerous health disorders (Okoye et al., 2021). This plant contains a variety of phytochemicals, including alkaloids, flavonoids, tannins, and saponins (Opoku and Akoto, 2015; Mollica et al., 2022), each linked with distinct therapeutic effects. These bioactive substances have been associated with antioxidant activities (Akinmoladun et al., 2007), anti-inflammatory responses (Akinawo et al., 2017), antimalarial properties (Atanu et al., 2021), antimicrobial effects (Adomi and Umukoro, 2010), and anticancer potential (Babatunde, 2017). Identification and measurement of these compounds have been achieved using analytical techniques such as High-Performance Liquid Chromatography (HPLC), Gas Chromatography–Mass Spectrometry (GC–MS), and standard phytochemical screening protocols (Byaruhanga, 2023). Studies on the stem bark have revealed the presence of major compounds such as steroids, terpenoids, alkaloids, saponins, tannins, and flavonoids, all of which contribute to the plant’s broad medicinal applications (Byaruhanga, 2023). Alkaloids from *A. boonei* possess analgesic, anti-inflammatory, and antimalarial actions, with mechanisms involving

modulation of pain pathways and regulation of immune processes, making them valuable in conditions such as inflammatory bowel disorders and gastrointestinal pain (Okoye et al., 2021). Flavonoids offer significant antioxidant capacity, which protects the intestinal mucosa from oxidative injury implicated in peptic ulcer formation and inflammatory bowel disease (Opoku and Akoto, 2015). Saponins, another key phytochemical class, display anti-diarrheal activities by influencing gastrointestinal motility and electrolyte transport, thereby assisting in the management of absorption-related disorders and intestinal infections (Josephine et al., 2024). Tannins present in high concentrations within the bark exhibit astringent properties that promote

epithelial tissue contraction, reduce excess secretions, and control local inflammation (Okorie et al., 2022). Experimental animal studies have shown that *A. boonei* bark extract can minimize epithelial erosion and promote mucosal repair following chemically induced intestinal damage (Okorie et al., 2022). In addition, in vitro findings indicate that extracts from this plant may enhance glucose uptake in intestinal epithelial cells, suggesting a possible role in improving nutrient absorption and metabolic control (Nkono et al., 2016).

## **2.5 Pharmacological Activities of *Alstonia boonei***

*Alstonia boonei* exhibits a broad spectrum of pharmacological activities attributed to its rich phytochemical constituents, including alkaloids, flavonoids, tannins, saponins, triterpenes, and phenolic compounds (Agbaje et al., 2022). The bark and leaves are particularly noted for their potent antioxidant activity, which is largely due to their high phenolic and flavonoid content (Akinmoladun et al., 2024). These antioxidants play a critical role in mitigating oxidative stress and protecting against cellular damage, thereby supporting the management of chronic conditions such as diabetes, hypertension, and cardiovascular disorders (Onoja et al., 2023). The plant demonstrates significant antimicrobial properties against a variety of pathogenic microorganisms, including *Escherichia coli*, *Staphylococcus aureus*, and *Candida albicans*, through both ethanolic and aqueous extracts (Eze et al., 2024).

In addition, *A. boonei* exhibits pronounced anti-inflammatory effects in experimental models by reducing edema and suppressing pro-inflammatory cytokines (Akinmoladun et al., 2024). Antidiabetic activity has also been reported, with extracts improving insulin sensitivity and lowering blood glucose levels in alloxan-induced diabetic rats (Onoja et al., 2023). The analgesic

properties of the bark are widely recognized in traditional medicine, where decoctions are used to relieve rheumatic pain, malaria-associated fever, and musculoskeletal discomfort (Ogundare et al., 2022). Furthermore, studies have shown its antimalarial potential through inhibition of *Plasmodium falciparum* growth and modulation of host immune response (Iwu et al., 2021). The plant's immunomodulatory effects are equally noteworthy, as *A. boonei* extracts enhance white blood cell count, stimulate macrophage activity, and regulate cytokine expression, supporting overall immune defense (Agbaje et al., 2022). Preliminary anticancer investigations suggest that the alkaloid fraction can induce apoptosis in tumor cells, inhibit angiogenesis, and disrupt cancer cell proliferation, although further clinical validation is required (Eze et al., 2024). Additional studies indicate hepatoprotective activity, where bark extracts ameliorate chemically induced liver damage by enhancing antioxidant enzyme activity and reducing lipid peroxidation (Akinmoladun et al., 2024). Collectively, these findings highlight *A. boonei* as a pharmacologically versatile species with considerable potential for the development of novel therapeutic agents and natural product-based pharmaceuticals.

### **2.5.1 Hepatoprotective Activity of *Alstonia boonei***

The hepatoprotective effects of *Alstonia boonei* have been widely documented in experimental models of chemically induced liver injury (Agbaje et al., 2022). Aqueous and methanolic extracts of the stem bark have demonstrated significant protection against carbon tetrachloride (CCl<sub>4</sub>), paracetamol, and alcohol-induced hepatotoxicity by normalizing serum liver enzyme activities and restoring histopathological architecture of liver tissues (Akinmoladun et al., 2024). These effects are largely attributed to the high concentrations of alkaloids, triterpenes, and polyphenolic compounds with potent free-radical scavenging and membrane-stabilizing properties (Onoja et al.,

2023). In treated animals, marked reductions in alanine aminotransferase (ALT), aspartate aminotransferase (AST), alkaline phosphatase (ALP), and lipid peroxidation were observed, accompanied by increases in endogenous antioxidant enzymes such as superoxide dismutase and catalase (Eze et al., 2024).

Further investigations revealed that *A. boonei* bark extract not only protects hepatocytes but also enhances hepatic regeneration by stimulating protein synthesis and reducing pro-inflammatory cytokines, including tumor necrosis factor-alpha and interleukin-6 (Ogundare et al., 2022). Its broad antioxidant synergy validates its traditional use in the management of jaundice and other liver disorders among West African populations (Agbaje et al., 2022). Importantly, both aqueous and ethanol extracts display a high safety margin when administered at therapeutic doses, with no evidence of acute or sub-chronic toxicity in rodent models (Akinmoladun et al., 2024).

Collectively, these findings support the potential of *Alstonia boonei* as a natural hepatoprotective agent, providing biochemical and histological evidence of liver protection and positioning the plant as a promising candidate for development into standardized herbal formulations.

### **2.5.2 Nephroprotective Activity of *Alstonia boonei***

The nephroprotective potential of *Alstonia boonei* is increasingly highlighted in ethnopharmacological and toxicological literature due to its diverse secondary metabolites and strong antioxidant profile (Onocha et al., 2019). Traditionally, different parts of the plant—particularly the stem bark and leaves—are used in African herbal medicine for the management of kidney-related disorders, malaria, and fever, suggesting a broad spectrum of therapeutic activity (Abosi and Raseroka, 2003). Phytochemical investigations reveal abundant

alkaloids, flavonoids, saponins, and phenolic compounds, which exhibit free radical–scavenging properties that mitigate oxidative stress and reduce inflammatory responses in renal tissues (Okoye et al., 2014). Experimental studies using animal models of nephrotoxicity have demonstrated that aqueous and ethanol extracts of *A. boonei* protect against chemically induced renal injury by lowering serum creatinine, blood urea nitrogen, and uric acid levels, while improving histopathological outcomes in the kidney (Akinmoladun et al., 2020). These effects are associated with modulation of oxidative enzymes, inhibition of lipid peroxidation, and stabilization of renal cell membranes (Eze et al., 2016).

Despite its promising renal benefits, attention to dosage and extract purity remains important, as excessive or poorly processed preparations may contain bioactive alkaloids capable of inducing cytotoxicity (Onocha et al., 2019). Continued pharmacological and toxicological evaluations are therefore essential to establish standardized safe doses, optimize extraction methods, and clarify molecular pathways underlying the nephroprotective action of *Alstonia boonei* for potential clinical application (Akinmoladun et al., 2020; Okoye et al., 2014)

### **Anatomy of the Liver**

The liver is the largest internal organ in the human body, located in the upper right quadrant of the abdominal cavity, just below the diaphragm and above the stomach, extending partially into the left upper quadrant (Moore et al., 2018). It weighs approximately 1.4–1.6 kg in adults and performs over 500 vital functions including metabolism, detoxification, protein synthesis, and bile production (Guyton and Hall, 2021). Structurally, the liver is divided into two main anatomical lobes right and left by the falciform ligament, although functionally, it is divided into eight

Couinaud segments, each with its own vascular inflow, outflow, and biliary drainage (Netter, 2014). The right lobe is significantly larger than the left, encompassing the caudate and quadrate lobes on the visceral surface (Snell, 2019). Blood from the portal vein and hepatic artery flows through sinusoids, allowing hepatocytes to absorb nutrients and detoxify substances before the blood drains into the central vein and eventually exits via the hepatic vein (Junqueira et al., 2015). The liver receives dual blood supply: approximately 75% from the hepatic portal vein (carrying nutrient-rich, oxygen-poor blood from the gastrointestinal tract) and 25% from the hepatic artery (carrying oxygen-rich blood). The biliary system, which begins in the canaliculi between hepatocytes, collects bile and channels it via progressively larger ducts to the common hepatic duct and eventually to the gallbladder or duodenum (Sherwood, 2016). The liver's capsule, known as Glisson's capsule, is a thin connective tissue layer that surrounds the organ and extends into the parenchyma to support the hepatic lobules (Standring, 2020). The entire organ is covered by visceral peritoneum, except at the bare area, which is in direct contact with the diaphragm.

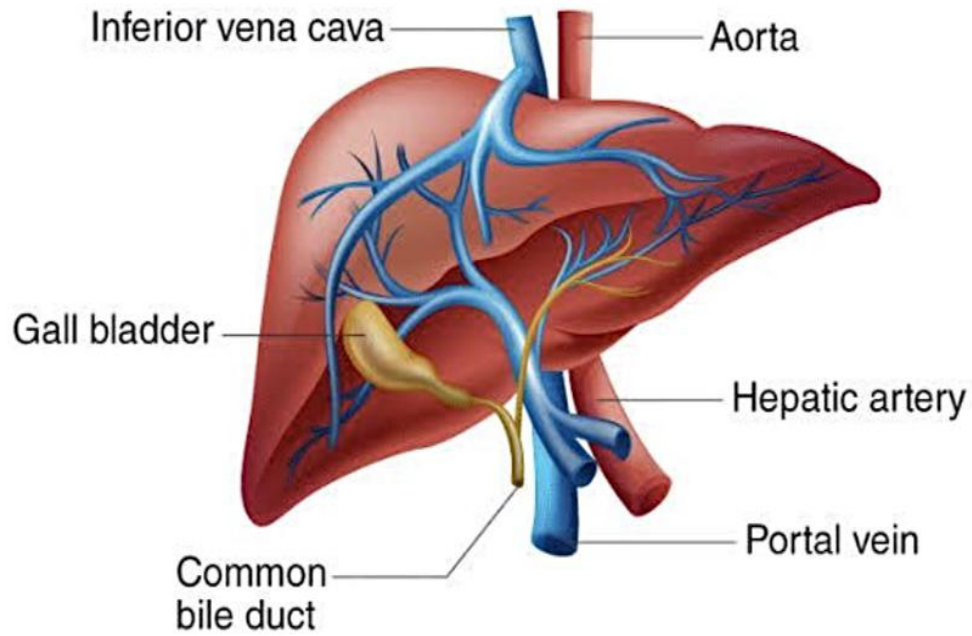


Figure 2.2 Anatomy of the Liver (Junqueira et al., 2015).

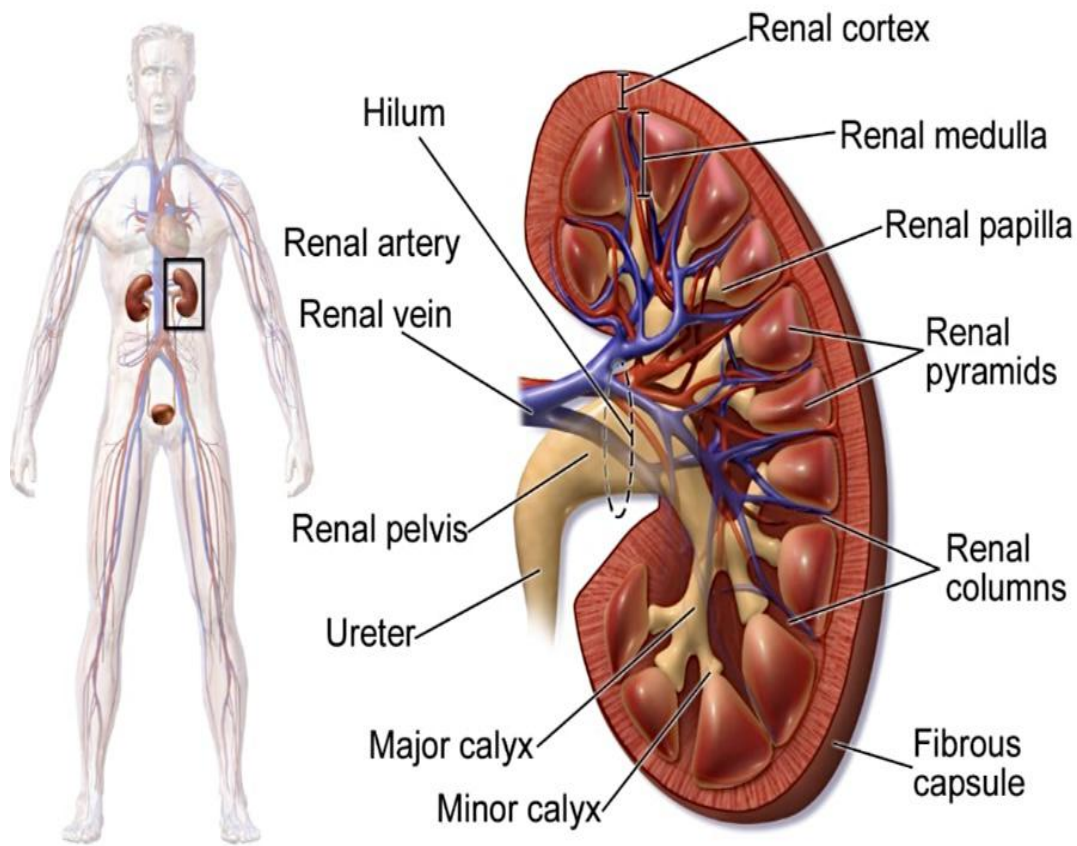
## **Anatomy of the Kidney**

The kidneys are vital excretory organs in the human body, responsible for the regulation of blood composition, waste excretion, electrolyte balance, and endocrine functions. Each kidney is a bean-shaped, reddish-brown organ located in the retroperitoneal space of the upper abdomen, flanking the vertebral column between the levels of the twelfth thoracic (T12) and third lumbar (L3) vertebrae. The right kidney sits slightly lower than the left due to the anatomical position of the liver (Moore, Dalley, and Agur, 2018). In adults, each kidney measures approximately 11 centimeters in length, 6 centimeters in width, and 3 centimeters in thickness, with an average weight of 120 to 150 grams (Snell, 2019). The external anatomy of the kidney reveals a convex lateral border and a concave medial border. The medial border features a distinct depression called the hilum, which serves as the entry and exit point for the renal artery, renal vein, lymphatics, nerves, and the ureter. Each kidney is enveloped by three protective layers: an inner fibrous renal capsule, a middle perirenal fat layer that cushions the organ, and an outer renal fascia that anchors the kidney to surrounding structures (Standring, 2020). Internally, the kidney is divided into two major regions: the outer renal cortex and the inner renal medulla. The cortex houses the glomeruli, proximal and distal convoluted tubules, and provides a granular appearance due to dense capillary networks. The medulla contains renal pyramids, which are cone-shaped structures whose apex, the renal papilla, empties urine into minor calyces. These calyces converge into major calyces, leading to the renal pelvis, which narrows into the ureter (Netter, 2014). These structural features facilitate the unidirectional flow of urine from the nephrons toward the bladder. The functional unit of the kidney is the nephron, and each kidney contains approximately 1 to 1.5 million of them. A nephron consists of a renal corpuscle (comprising the glomerulus and Bowman's capsule) and a renal

tubule, which is subdivided into the proximal convoluted tubule, the loop of Henle, the distal convoluted tubule, and the collecting duct. The renal corpuscle is the initial site of filtration, where blood plasma is filtered through the glomerular capillaries into Bowman's space. This filtrate is subsequently modified through reabsorption and secretion along the tubular segments to form urine (Junqueira, Carneiro, and Kelley, 2015). The kidneys are highly vascularized, receiving about 20–25% of the cardiac output. The renal artery, a direct branch of the abdominal aorta, enters the kidney at the hilum and branches into segmental, interlobar, arcuate, and interlobular arteries. These further supply the glomerular capillaries, facilitating efficient blood filtration. Filtered blood exits through the renal vein, which drains directly into the inferior vena cava (Guyton and Hall, 2021).

Apart from filtration, the kidneys also perform essential endocrine functions. They produce erythropoietin, which stimulates red blood cell production in the bone marrow, and renin, a hormone critical in the regulation of blood pressure via the renin-angiotensin-aldosterone system.

Additionally, they are involved in the activation of vitamin D to its bioactive form, calcitriol, which is important for calcium homeostasis (Sherwood, 2016)



## Kidney Anatomy

Figure 2.3 Anatomy of the kidneys (Junqueira et al., 2015).

## **Physiology of the Liver**

The liver is the largest gland in the human body and is responsible for a vast array of physiological functions. One of its primary roles is carbohydrate metabolism, where it regulates blood glucose levels through glycogenesis (conversion of glucose to glycogen), glycogenolysis (breakdown of glycogen), and gluconeogenesis (generation of glucose from non-carbohydrate sources) (Guyton and Hall, 2021). In lipid metabolism, the liver synthesizes triglycerides, cholesterol, phospholipids, and lipoproteins. It also plays a central role in the oxidation of fatty acids, particularly during prolonged fasting or low carbohydrate intake. The liver is also the main site for protein metabolism, including deamination of amino acids, urea formation, and plasma protein synthesis such as albumin, clotting factors, and globulins (Junqueira et al., 2015). One of the most critical liver functions is detoxification. Hepatocytes metabolize endogenous waste products like ammonia into urea and also process exogenous toxins such as drugs and alcohol through enzymatic biotransformation, primarily via the cytochrome P450 system (Sherwood, 2016). The liver also contributes to bile production, essential for fat emulsification and absorption in the small intestine. Bile is composed of bile salts, bilirubin, cholesterol, and electrolytes. The liver continuously secretes bile, which is stored and concentrated in the gallbladder and released into the duodenum postprandially (Moore et al., 2018). Moreover, the liver functions as a storage organ, preserving vitamins (A, D, B12), minerals (iron, copper), and glycogen. It also plays an important endocrine role, converting inactive thyroid hormone (T4) into its active form (T3), and metabolizing steroid hormones and insulin (Snell, 2019).

## **Physiology of the Kidney**

The kidneys serve as the body's primary excretory and regulatory organs, ensuring the internal environment remains stable despite external changes. Their chief role is filtration of blood to produce urine. This process begins in the glomerulus, where hydrostatic pressure forces plasma through a semi-permeable membrane into Bowman's capsule, initiating the formation of filtrate (Guyton and Hall, 2021). Following filtration, the nephron performs selective reabsorption and secretion. In the proximal convoluted tubule, approximately 65–70% of sodium, water, glucose, amino acids, and bicarbonate are reabsorbed into the bloodstream. The loop of Henle, particularly the ascending limb, plays a key role in urine concentration via a countercurrent mechanism (Sherwood, 2016). The distal convoluted tubule and collecting duct fine-tune electrolyte and fluid balance. Aldosterone promotes sodium reabsorption and potassium excretion, while antidiuretic hormone (ADH) regulates water reabsorption based on plasma osmolality. The result is the formation of concentrated or dilute urine depending on physiological needs (Moore et al., 2018). The kidneys are essential in acid-base regulation, by reabsorbing bicarbonate and secreting hydrogen ions to maintain blood pH within the physiological range (7.35–7.45). In addition to these functions, the kidneys are a major site of endocrine activity. They release erythropoietin, which stimulates red blood cell production in response to hypoxia, and renin, which regulates blood pressure via the renin-angiotensin-aldosterone system (Standring, 2020). They contribute to vitamin D metabolism, converting calcidiol to its active form, calcitriol, which promotes calcium and phosphate absorption in the intestines and bone mineralization (Junqueira et al., 2015).

## CHAPTER THREE

### MATERIALS AND METHODS

#### 3.1 MATERIALS, REAGENTS AND EQUIPMENT FOR RESEARCH

##### 3.1.1 Materials

Materials used in the course of research include: Cages, Water bowls, Feeding bowls, Rat feed, Buckets, Gloves, Facemasks, Measuring cylinders, Beakers, Universal bottles, Empty water bottles, Spatulas, Dissecting sets, Disinfectants, Syringes, Oral gavage needles, Cotton wools, Knives, Scissors, Towels, Sponges, Masking tape

##### 3.1.2 Reagents Used

They include: Chloroform, Formalin, Distilled water, Gentian violet, Normal saline

##### 3.1.3 Equipment Used

They include: Weigh balance, Blender, Freeze dryer, Refrigerator

##### 3.1.4 Reagents And Chemicals

The following chemical reagents were utilized during the histological preparation and staining procedures: Haematoxylin dye (Merck KGaA, Darmstadt, Germany), Eosin Y dye (Sigma-Aldrich, St. Louis, MO, USA), 1% acid-alcohol (prepared in-house using absolute ethanol and concentrated HCl, BDH Chemicals Ltd., Poole, UK), Xylene (Fisher Scientific, Loughborough, UK), Dibutylphthalate Polystyrene Xylene (DPX) mounting medium (Loba Chemie Pvt. Ltd., Mumbai, India), 10% Formalin (Leica Biosystems, Wetzlar, Germany), and normal saline solution

(J.T. Baker, Phillipsburg, NJ, USA). All reagents were of analytical grade and distilled before use to ensure purity and consistency.

### **3.2 Collection of Experimental Plant Materials**

Fresh *Alstonia boonei* stem bark were harvested from the Ekosodin community in Ovia Northeast Local Government Area of Edo State.

#### **3.2.1 Identification and Authentication**

Prof. H.A. Akinnibosun of the Department of Plant Biology and Biotechnology, Faculty of Life Science, University of Benin, identified and authenticated the *Alstonia boonei* stem bark from the family of Apocynaceae and assigned a Voucher Number: UBH-A343.

#### **3.2.2 Preparation of Plant Material**

The aqueous extract of *Alstonia boonei* stem bark was prepared at the Department of Pharmacognosy, University of Benin. Fresh stem bark of *Alstonia boonei* were thoroughly washed and air-dried at room temperature. The dried material was pulverized into fine powder using a mechanical grinder (Marlex ExcellaMG10, India).

A total of 500 g of the powdered sample was soaked in 1.5 L of distilled water for 24 hours. During this period, the mixture was intermittently stirred using a sterile glass rod to facilitate extraction. Subsequently, the solution was blended for 15 minutes with an electric blender and then gently heated until steam emission was observed. The mixture was stored overnight in a Westcool refrigerator at 4 °C. It was then filtered using clean muslin cloth, and the resulting filtrate was concentrated under reduced pressure at 40 °C using a rotary evaporator. Final moisture

removal was done by freeze-drying to obtain a dry extract of *Alstonia boone* which was stored in a refrigerator until use [Adebayo et al., 2019].

### **3.3 Animal Housing**

Twenty-four (24) Adult male and female albino rats of comparable sizes and average weight of 151.25g was procured from the animal farm, Histopathology Laboratory Department of Benson Idahosa University, Benin, Edo State and transferred to the experimental Histopathology Laboratory Department, where there was one week of acclimatization. They were kept in wire mesh cages with tripod that separates the animal from its faeces to prevent contamination. During this period of acclimatization, the rats were fed with Growers' mash and water ad libitum. The rats was maintained according to international guidelines for handling experimental animals as reported by the Institute for Laboratory Animal Research (NRC, 1996). The experimental rats were divided into six groups (A – F). Each group contains four rats each ( $n = 4$ ). Group A served as the positive control, Group B-F served as the test groups.

### **3.4 Ethical Approvals**

Ethical approval was sought from the Ethics and Research Committee of the Ministry of Agriculture and Food Security for the protocol of this study with reference number, MAFSAEC: 025-12/08/0050. All of the experimental rats were handled according to international guidelines for handling experimental animals as reported by the Institute for Laboratory Animal Research (NRC, 1996).

### **3.5 Methodology**

#### **3.5.1 Experimental Design**

The rat were divided into 6 groups, each comprising of four rats each.

##### **Group A (n = 4 rats)**

This group served as control. Three male and one female rat on a separate cage. Rats were fed pelleted vita finisher feed and water for fourteen (14) consecutive days.

##### **Group B (n = 4 rats)**

Four female rats were administered *Alstonia boonei* stem bark extract 100mg/kg body weight orally in addition to vita feed and water ad libitum for fourteen (14) consecutive days).

##### **Group C (n = 4 rats)**

Four female rats were administered *Alstonia boonei* stem bark extract 200mg/kg body weight orally in addition to vita feed and water ad libitum for fourteen (14) consecutive days.

##### **Group D (n = 4 rats)**

Four female rats were administered *Alstonia boonei* stem bark extract 400mg/kg body weight orally in addition to vita feed and water ad libitum for fourteen (14) consecutive days.

##### **Group E (n = 4 rats)**

Four female rats were administered *Alstonia boonei* stem bark extract 600mg/kg body weight orally in addition to vita feed and water ad libitum for fourteen (14) consecutive days.

### Group F (n = 4 rats)

Four female rats were administered *Alstonia boonei* stem bark extract 800mg/kg body weight orally in addition to vita feed and water ad libitum for fourteen (14) consecutive days.

At the end of the 28-day treatment period, all animals were humanely euthanized by cervical dislocation in according to international guidelines for handling experimental animals as reported by the Institute for Laboratory Animal Research (NRC, 1996). A longitudinal incision was made from the pelvic region to the thoracic cavity to expose

the internal organs. Fixation was carried out for a minimum of 24 hours to ensure adequate tissue penetration and preservation (Bancroft and Gamble, 2008; Kiernan, 2008).

### 3.5.2 Experimental grouping and dosage administration of *Alstonia boonei* stem bark extract on rats.

| S/N | GROUPING | ADMINISTRATION   |
|-----|----------|--|
| A   | 4        | Control- Feed and distilled water only                       |
| B   | 4        | dose of 100mg/kg of <i>Alstonia boonei</i> stem bark extract |
| C   | 4        | dose of 200mg/kg of <i>Alstonia boonei</i> stem bark extract |
| D   | 4        | dose of 400mg/kg of <i>Alstonia boonei</i> stem bark extract |
| E   | 4        | dose of 600mg/kg of <i>Alstonia boonei</i> stem bark extract |
| F   | 4        | dose of 800mg/kg of <i>Alstonia boonei</i> stem bark extract |

### 3.5.3 Dosage Calculations

#### GROUP B

Using 200mg/kg body weight; Each rat was weighed

$$200\text{mg} = 1\text{kg}$$

$$200\text{mg} = 1000\text{g}$$

$$X\text{mg} = \text{weight of rat in g}$$

$$X\text{mg} = \frac{20\text{mg} \times \text{weight of rat (g)}}{1000}$$

Using 1g dissolved in 10ml

If 10000mg is dissolved in 10ml, Xmg will contain how many ml?

Therefore;

$$X\text{ml} = \frac{X\text{mg} \times 10\text{ml}}{10000\text{mg}}$$

Note : The same calculation goes for Group C-200mg/kg and Group D-400mg/kg. The weight of each Rat was checked on a weekly basis to determine the new dosage for each Rat.

### 3.6 Histopathological Studies

At the end of the experiment, four (4) rats from each group (one female and three male rats for Groups A, while four female rats from Groups B - F, were humanely euthanized via cervical dislocation, 24 hours after the last day of administration. The Liver and Kidney tissues were

harvested for Groups A, B, C, D, E and F for the experiment using a sterile surgical blade and examined for ulceration or inflammation (Bancroft et al., 2019).

### **3.6.1 Histological Technique**

#### **Procedure:**

Histopathologically, to detect inflammation, the whole organ (that is the Liver and kidney tissues) were autopsied, stained using hematoxylin and eosin staining techniques to demonstrate general tissue structure and then viewed microscopically. The procedure involved includes:

Tissue (the Liver and kidney tissues) processing using automatic method. Sequences for automatic tissue processing were as follows:

Harvesting Tissue: The required tissues (Liver and kidney tissues) were

harvested from the rats and immediately put in a fixative. All parts of the required tissue that showed obvious microscopic changes were essentially selected for sampling. Tissues were cut into thin slices of 3mm by size.

Selection of Tissue: The Liver and kidney tissues were selected for histological assessment due to their essential roles in digestion, absorption, immune defense, and their high vulnerability to toxicological and pharmacological insults.

Fixation: The fixation in a 10% neutral buffered formalin (NBF) solution. This fixative was prepared from commercially available formalin (37–40% formaldehyde), tap water, sodium dihydrogen phosphate monohydrate, and disodium hydrogen phosphate anhydrous. The

buffering system maintained a near-neutral pH (~7.0), which is essential for preventing formalin pigment artifacts and preserving cellular detail (Bancroft and Gamble, 2008). Tissue specimens were immersed in the fixative for a minimum of 24 hours at room temperature to ensure complete penetration and stabilization of the Liver and kidney tissue architecture, which is particularly delicate due to its mucosal complexity and high enzymatic activity.

Following fixation, the tissues were subjected to graded dehydration through a series of ethanol solutions with increasing concentrations. The tissues were immersed sequentially in 70%, 90%, and 95% ethanol, followed by three changes of absolute alcohol, each for 2 hours. The alcohol volume used was approximately 50–100 times the tissue volume to ensure effective dehydration and minimize tissue distortion.

After dehydration, the tissues underwent clearing in two changes of xylene, each lasting 90 minutes. Xylene served to remove the alcohol and render the tissue receptive to paraffin wax. Subsequently, impregnation with molten paraffin wax was performed in two stages, each for 2 hours, at the melting point of paraffin. The wax volume was maintained at 25–30 times that of the tissues to ensure thorough infiltration and structural integrity. Once impregnated, the tissues were embedded in labeled tissue cassettes filled with fresh molten wax, which was allowed to settle and solidify. The solidified blocks were then rapidly cooled in cold water to stabilize them. Finally, each block was trimmed and sectioned using a digital rotary microtome (Histoline MR3000, Italy) into thin slices suitable for staining and microscopic (Bancroft and Gamble, 2008).

### **Staining of Processed Tissues**

Tissue sections prepared for general histological evaluation were stained using the

Ehrlich's Haematoxylin and Eosin (HandE) staining technique, following the method outlined by Archibong et al. (2021).

**Principle:** Hematoxylin is a basic dye and thus has affinity for the acidic part of the cellular component which is the nucleus. Therefore, the nucleus stains blue while eosin on the other hand is an acidic dye thus has affinity for the basic component of the cells which is the cytoplasm therefore it stains it pink which is the color of the dye. This staining procedure was facilitated with a mordant that linked the stain to the tissue and a differentiator (acid alcohol) that differentiated the nuclear stain from cytoplasmic stain.

### **Procedure For Hematoxylin And Eosin Staining**

Initially, the paraffin-embedded sections were dewaxed by immersing the slides in two changes of xylene for 2 minutes each to remove the embedding medium. The slides were then rehydrated through a series of descending ethanol concentrations, beginning with absolute alcohol for 2 minutes, followed by 90% and 70% ethanol, each for 1 minute. After rehydration, the slides were rinsed under running tap water for 1 minute to remove excess alcohol and prepare the tissue for staining. The tissue sections were then stained with hematoxylin for 10 minutes, enabling nuclear structures to take up a blue-purple color. The slides were subsequently rinsed in distilled water for 30 seconds and differentiated in 1% acid alcohol for 15 seconds to remove excess hematoxylin and sharpen nuclear detail. This was followed by a 5-minute rinse in distilled water to neutralize the acid. The sections were then counterstained with 1% eosin for 5 minutes, which imparted a pink to red coloration to the cytoplasm and connective tissues. After counterstaining, the slides were rinsed under running tap water for 30 seconds. Dehydration was then carried out by passing the sections

through ascending concentrations of alcohol (70%, 90%, and 100%), each for 1 minute, to remove residual water. This was followed by clearing in two changes of xylene for 2 minutes each. Finally, the sections were mounted with DPX mounting medium, covered with a coverslip, and allowed to dry. The prepared slides were examined microscopically using objective lenses to assess histological features (Archibong et al., 2021).

### **3.7. Microscopy And Photomicrography**

Tissue sections were examined at 40× and 100× magnifications using an Olympus CX23 binocular light microscope, equipped with an integrated LED illumination system to ensure consistent and high-contrast visualization of histological features. For image documentation, photomicrographs were captured using an Olympus BX53 trinocular microscope fitted with an Olympus DP74 high-resolution digital camera. The setup was connected to a computer via Olympus cell Sens imaging software, which facilitated accurate acquisition and processing of the microscopic images.

#### **3.7.1 Statistical Analysis**

The mean and standard deviation were used to express all weight results. Statistical programs for Social Sciences (SPSS) version 20 were used to conduct the statistical analysis on weight of the rats, liver and kidney organs as well as Liver function Test and Kidney function Test analysis.

## CHAPTER FOUR

### RESULTS

#### 4.1 HISTOPATHOLOGICAL EXAMINATION

The following are the histological findings observed in the course of investigating the kidney and liver tissue after administering different doses of *Alstonia boonei* stem bark extract (group A= control, group B= 100 mg/kg, group C= 200 mg/kg, group D= 400 mg/kg, group E= 600mg/kg, group F= 800mg/kg):

##### 4.1.1 Liver

Section of the liver from the control rats showed hepatocytes with eosinophilic cytoplasm surrounding a centrally placed normochromic nucleus with indistinct nucleoli. The hepatocytes were arranged in cords separated by clear, non-congested sinusoids with abundant eosinophilic cytoplasm arranged in radial cords around patent hepatic sinusoids. Each cell contained a centrally placed normochromic nucleus with indistinct nucleoli, and no visible signs of inflammation, necrosis, or congestion were observed. **(Plate 4.1A & 4.1B)**

Section of the liver from rats administered low-dose *Alstonia boonei* stem bark extract showed preserved hepatic structure with mildly swollen hepatocytes with granular eosinophilic cytoplasm and prominent, centrally placed normochromic nuclei. Mild sinusoidal dilation and mild cytoplasmic swelling was observed with otherwise preserved hepatic architecture. **(Plate 4.2A & 4.2B)**

Section of the liver from rats administered a higher dose of *Alstonia boonei* stem bark extract

showed dilated hepatic sinusoids and hepatocytes with vacuolated eosinophilic cytoplasm, some appearing mildly distorted. The nuclei were visible and centrally placed but slightly irregular in shape and showed occasional chromatin condensation. **(Plate 4.3A & 4.3B)**

Section of the liver showed moderate distortion of hepatic architecture, hepatocytes (arrow) with eosinophilic cytoplasm, some appearing vacuolated and slightly disorganized. The hepatic cords appear narrowed, with dilated sinusoids and occasional mildly hyperchromatic pyknotic nuclei visible. No widespread necrosis is seen, but there is evidence of mild to moderate hepatocellular degeneration. **(Plate 4.4A & 4.4B)**

Section of the liver from rat administered 600 mg/kg of *Alstonia boonei* stem bark shows hepatocytes (arrow) with mildly eosinophilic cytoplasm and centrally placed normochromic nuclei. Hepatic cords appear preserved, with slightly dilated sinusoids. No significant necrosis, inflammation, or cellular degeneration is observed. While section from the second rat revealed distorted hepatic architecture with marked hepatocellular degeneration. Hepatocytes (arrow) showed cytoplasmic vacuolation, eccentric and hyperchromatic nuclei, and loss of cell-to-cell boundaries. There is mild sinusoidal dilatation and congestion, indicating toxic hepatocellular injury. **(Plate 4.5A & 4.5B)**

Section of the liver from rat administered 800 mg/kg of *Alstonia boonei* stem bark shows hepatocytes with eosinophilic cytoplasm and mildly pleomorphic nuclei. There is evidence of sinusoidal dilatation and mild disruption in hepatic cord arrangement. However, no overt necrosis or inflammatory infiltrate is observed. Section of the liver from Rat B group F showed hepatocytes (arrow) with mildly eosinophilic cytoplasm and some areas of cellular distortion with slight

infiltration of inflammatory cells.(**Plate 4.6A & 4.6B**)

#### **4.1.2 Kidney**

Section of the kidney from control rats showed intact glomeruli with well-preserved Bowman's capsule and renal tubules lined by cuboidal epithelium with distinct nuclei. Sections showed intact glomeruli with well-defined capillary loops and normal Bowman's space. The renal tubules displayed cuboidal epithelium with clear cytoplasm and centrally placed nuclei.(**Plate 4.1C & 4.1D**)

Section of the kidney from rats in group B showed intact glomeruli with normal cellularity and patent Bowman's space. The surrounding renal tubules exhibited normal cuboidal epithelium with preserved brush borders and preserved epithelial lining with no evident cellular degeneration or necrosis.(**Plate 4.2C & 4.2D**)

Section of the kidney from rats in group C showed well-defined glomerular tufts and normal renal corpuscles with normal cellularity and intact Bowman's space. The surrounding and adjacent renal tubules exhibited preserved epithelial lining with no signs of tubular degeneration or necrosis.  
(**Plate 4.3C & 4.3D**)

The kidney section from group D administered 400mg/kg of *Alstonia boonei* stem bark shows glomeruli (large arrow) with slight congestion and mild enlargement, but overall preserved architecture. The surrounding renal tubules (small arrow) appear mostly intact with minimal tubular epithelial cell swelling. There is mild interstitial inflammation indicated by scattered inflammatory cells (small arrow at the upper left).(Plate 4.4C & 4.4D)

Section of the kidney from Rat A showed a renal corpuscle (arrow) with mildly hypercellular

glomeruli and focal mesangial prominence. The surrounding tubules (arrow) revealed patchy epithelial degeneration with widened tubular lumens and interstitial infiltration by inflammatory cells. Section of the kidney from Rat B showed a mildly hypercellular glomerulus (arrow) with preserved architecture. The surrounding renal tubules (arrow) appeared mostly intact, though with occasional tubular dilation and sparse interstitial spaces.**(Plate 4.5C & 4.5D)**

Section of the kidney from Rat A showed distorted renal architecture with a glomerulus exhibiting marked hypercellularity and congestion. The surrounding renal tubules appeared dilated with flattened epithelial lining and extensive interstitial spaces. Section of the kidney from Rat B revealed a severely altered glomerulus with loss of structural detail and marked cellular infiltration. Tubular structures showed widespread epithelial degeneration, vacuolization, and interstitial edema.**(Plate 4.6C & 4.6D)**

**GROUP A (control):**

**Liver:**

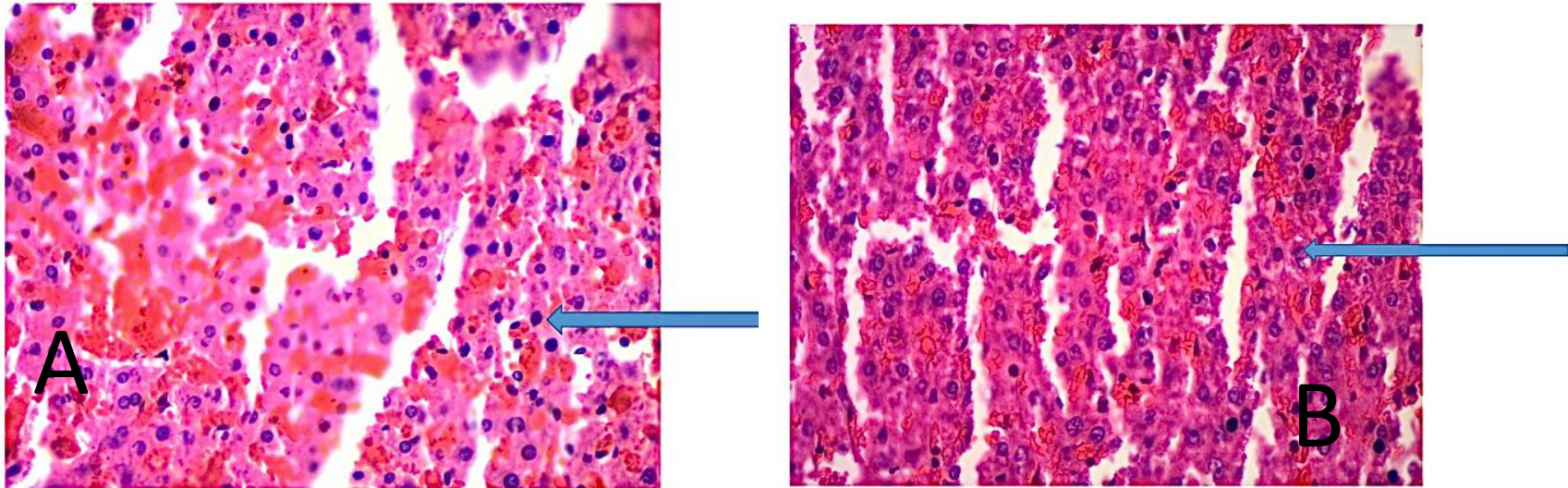


**Plate 4.1A:** Section of the liver from the control rats showed hepatocytes (arrow) with eosinophilic cytoplasm surrounding a centrally placed normochromic nucleus with indistinct nucleoli. The hepatocytes were arranged in cords separated by clear, non-congested sinusoids.

**FEATURES IN KEEPING WITH NORMAL HEPATOCYTES. H and E. Mag x400**

**Plate 4.1B:** Section of the liver from the control rat showed hepatocytes (arrow) with abundant eosinophilic cytoplasm arranged in radial cords around patent hepatic sinusoids. Each cell contained a centrally placed normochromic nucleus with indistinct nucleoli, and no visible signs of inflammation, necrosis, or congestion were observed. **FEATURES IN KEEPING WITH NORMAL HEPATOCYTES. H and E. Mag x400.**

**Kidney:**

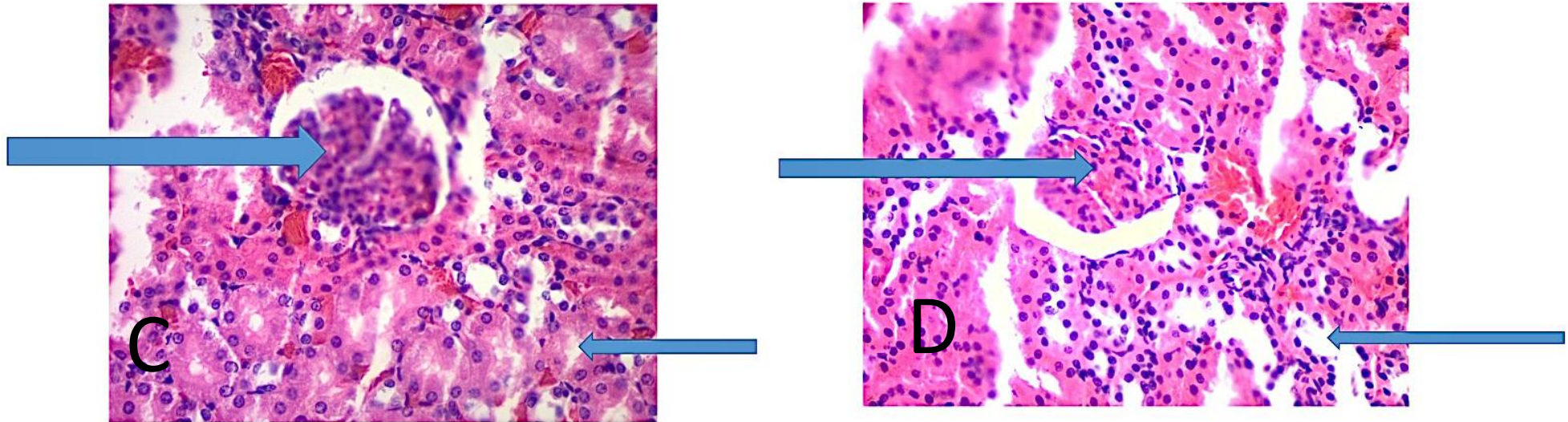


**Plate 4.1C:** Section of the kidney from control rats showed intact glomeruli (left arrow) with well-preserved Bowman's capsule and renal tubules (right arrow) lined by cuboidal epithelium with distinct nuclei. **FEATURES IN KEEPING WITH NORMAL RENAL HISTOLOGY.**

**H and E. Mag x400.**

**Plate 4.1D:** Section of the kidney from the control group showed intact glomeruli (large arrow) with well-defined capillary loops and normal Bowman's space. The renal tubules (small arrow) displayed cuboidal epithelium with clear cytoplasm and centrally placed nuclei. **FEATURES**

**IN KEEPING WITH NORMAL RENAL HISTOARCHITECTURE. H and E. Mag x400.**

**GROUP B (100mg/kg):**

**Liver:**

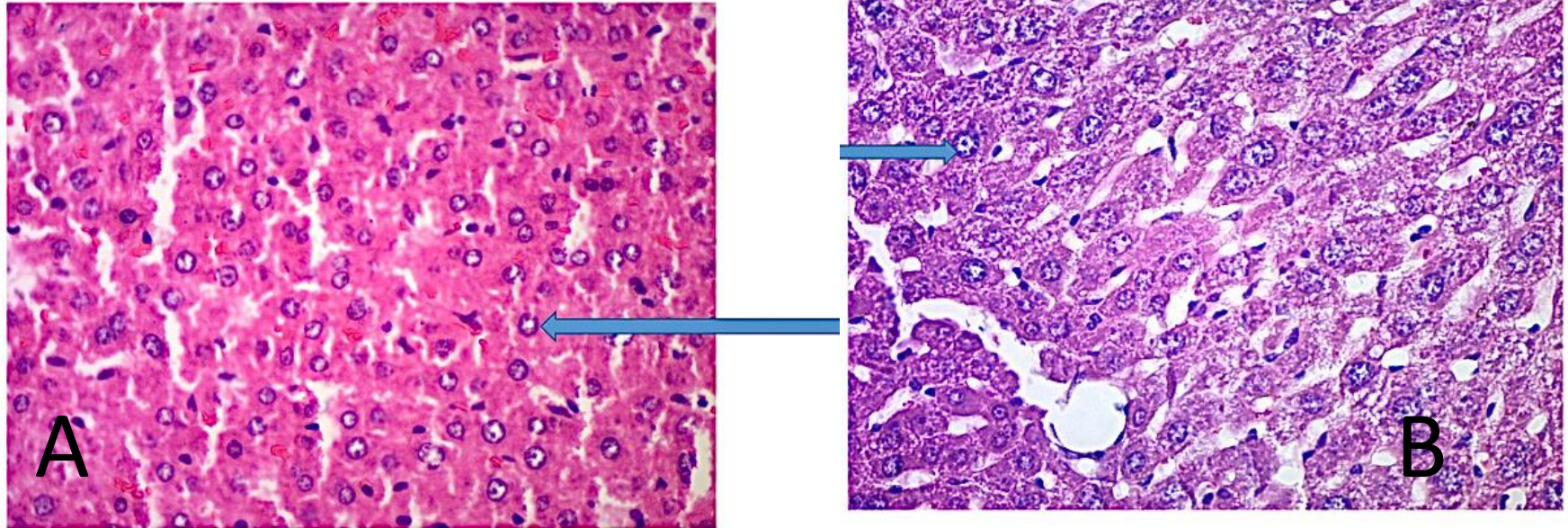


**Plate 4.2A:** Section of the liver from rats administered low-dose *Alstonia boonei* stem bark extract showed mildly swollen hepatocytes with granular eosinophilic cytoplasm and prominent, centrally placed nuclei. Mild sinusoidal dilation was observed with otherwise preserved hepatic architecture. **FEATURES SUGGESTIVE OF MILD HEPATOCELLULAR REACTIVE CHANGES. H and E. Mag x400**

**Plate 4.2B:** Section of the liver from rats administered low-dose *Alstonia boonei* stem bark extract showed preserved hepatic architecture with hepatocytes (arrow) exhibiting mildly eosinophilic cytoplasm and centrally placed normochromic nuclei. Sinusoids appeared slightly dilated, and mild cytoplasmic swelling was observed in some hepatocytes. **FEATURES SUGGESTIVE OF MILD HEPATOCELLULAR REACTIVE CHANGES. H and E. Mag x400**

**Kidney:**

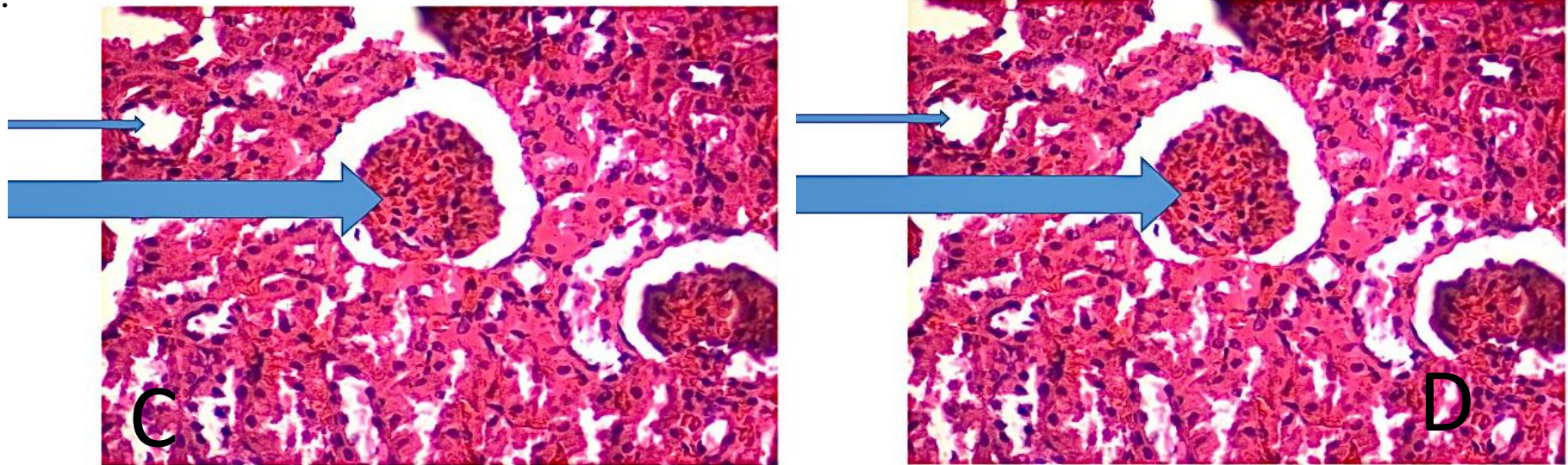


**Plate 4.2C:** Section of the kidney from rats in group B showed intact glomeruli (large arrow) with normal cellularity and patent Bowman's space. The surrounding renal tubules (small arrow) exhibited normal cuboidal epithelium with preserved brush borders. **FEATURES IN KEEPING WITH NORMAL RENAL HISTOLOGY. H and E. Mag x400.**

**Plate 4.2D:** Section of the kidney shows normal glomerulus (large arrow) with intact capillary loops and well-defined Bowman's space. The surrounding renal tubules (small arrow) exhibit preserved epithelial lining with no evident cellular degeneration or necrosis. **FEATURES IN KEEPING WITH NORMAL RENAL HISTOLOGY. H and E. Mag x400.**

**GROUP C (200mg/kg):**

**Liver:**

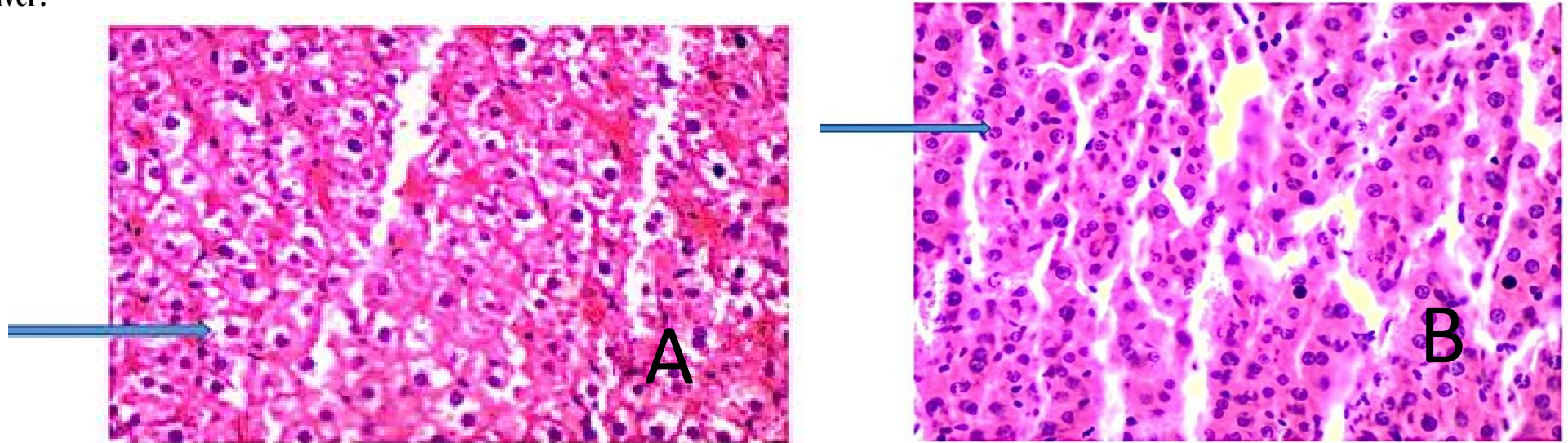


**Plate 4.3A:** Section of the liver from rats administered a higher dose of *Alstonia boonei* stem bark extract showed dilated hepatic sinusoids and hepatocytes (arrow) with vacuolated eosinophilic cytoplasm, some appearing mildly distorted. The nuclei were centrally placed but showed occasional chromatin condensation. **FEATURES IN KEEPING WITH MODERATE HEPATOCELLULAR DEGENERATION. H and E. Mag x400.**

**Plate 4.3B:** Section of the liver from rats administered higher-dose *Alstonia boonei* extract revealed dilated sinusoids, hepatocytes with vacuolated cytoplasm, and distortion of hepatic cords. Nuclei were still visible but slightly irregular in shape, with scattered chromatin condensation. **FEATURES IN KEEPING WITH MODERATE TUBULAR DEGENERATION. H and E. Mag x400.**

**Kidney:**

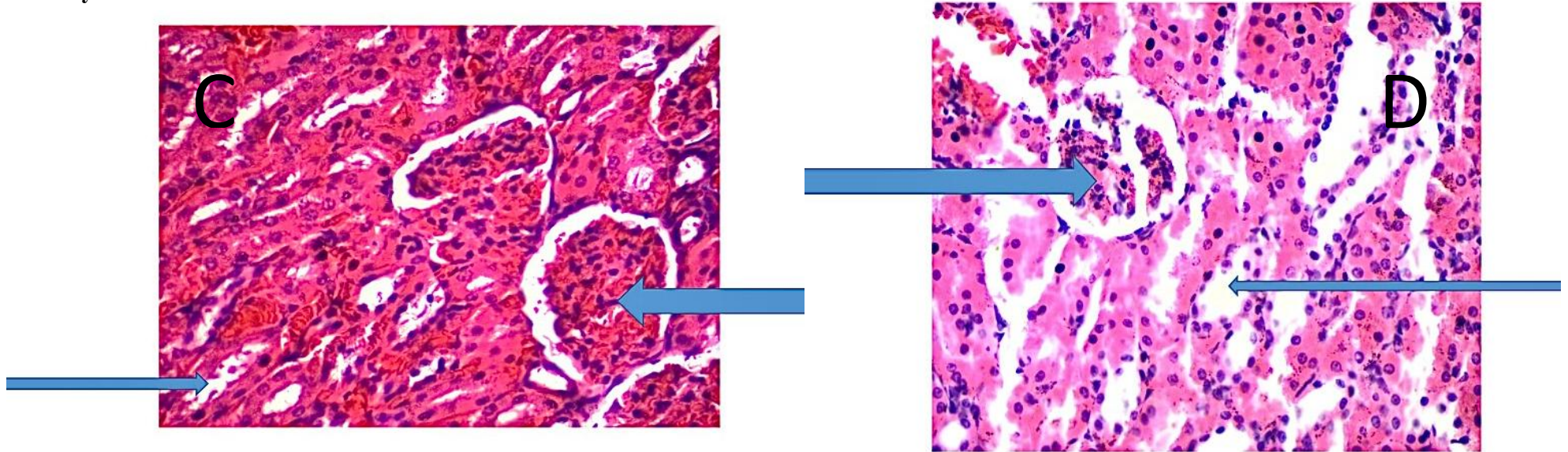


**Plate 4.3C:** Section of the kidney from rats in group C showed well-defined glomeruli (large arrow) with normal cellularity and intact Bowman's space. The adjacent renal tubules (small arrow) exhibited preserved epithelial lining with no signs of degeneration or necrosis. **FEATURES CONSISTENT WITH NORMAL RENAL HISTOLOGY. H and E. Mag x400.**

**Plate 4.3D:** Section of the kidney from rats in group C showed normal renal corpuscles (large arrow) with intact glomerular tufts and well-defined Bowman's capsules. The surrounding renal tubules (small arrow) exhibited preserved epithelial lining with no evidence of tubular degeneration or necrosis. **FEATURES CONSISTENT WITH NORMAL RENAL HISTOLOGY. H and E. Mag x400.**

**GROUP D (400mg/kg):**

**Liver:**

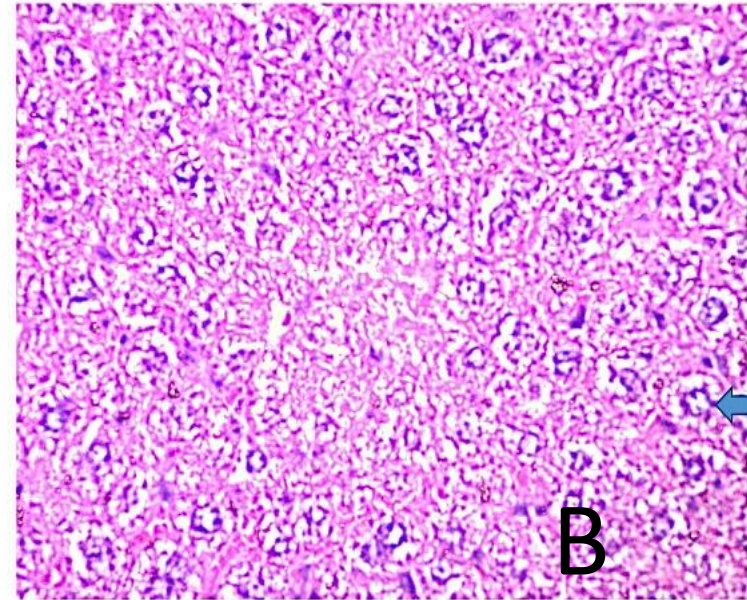
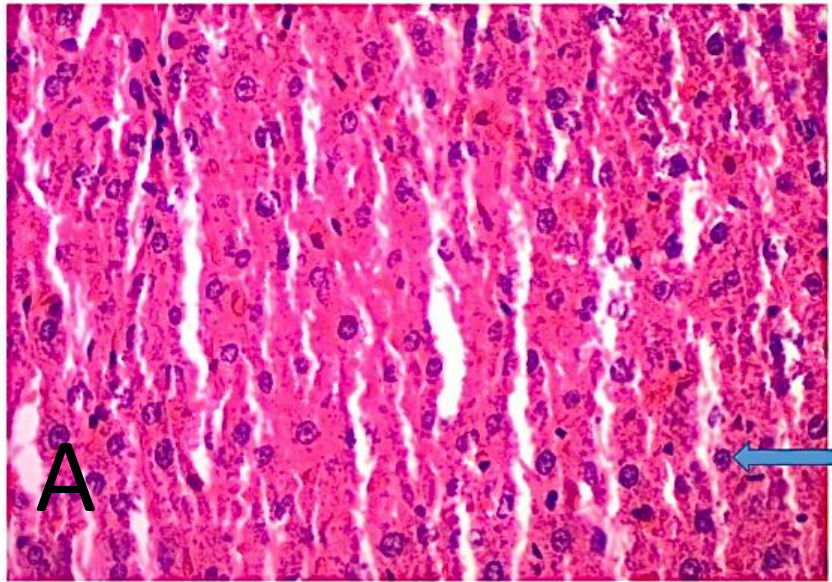


**Plate 4.4A:** Section of the liver showed hepatocytes (arrow) with eosinophilic cytoplasm, some appearing vacuolated and slightly disorganized. The hepatic cords appear narrowed, with dilated sinusoids and occasional pyknotic nuclei visible. No widespread necrosis is seen, but there is evidence of mild to moderate hepatocellular degeneration. **FEATURES SUGGESTIVE OF MODERATE HEPATOCELLULAR REACTIVE CHANGES WITH EARLY DEGENERATIVE FEATURES. H and E. Mag x400**

**Plate 4.4B:** Section of the liver from rats administered 400 mg/kg of *Alstonia boonei* stem bark extract showed moderate distortion of hepatic architecture, with hepatocytes (arrow) exhibiting cytoplasmic vacuolation and loss of cellular boundaries. The nuclei appeared mildly hyperchromatic, with areas showing sinusoidal dilatation and moderate hepatocellular degeneration. **FEATURES IN KEEPING WITH MODERATE DEGENERATIVE CHANGES. H and E. Mag x400**

**Kidney:**

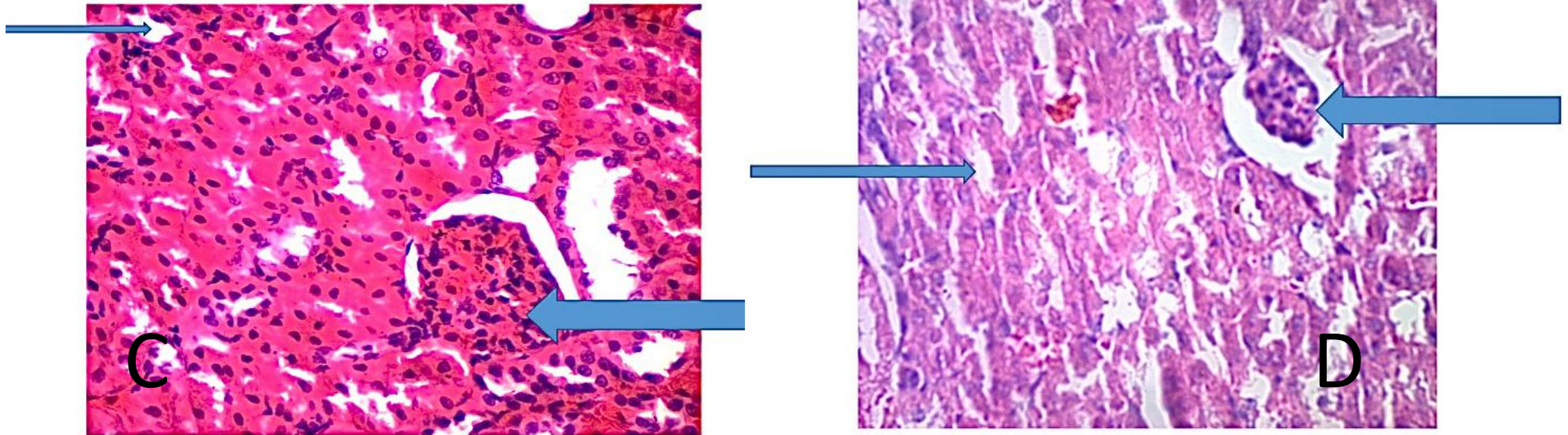


**Plate 4.4C:** The kidney section from group D shows glomeruli (large arrow) with slight congestion and mild enlargement, but overall preserved architecture. The surrounding renal tubules (small arrow) appear mostly intact with minimal tubular epithelial cell swelling. There is mild interstitial inflammation indicated by scattered inflammatory cells (small arrow at the upper left). **FEATURES SUGGEST MILD RENAL TISSUE RESPONSE POSSIBLY DUE TO TREATMENT OR EARLY SIGNS OF RENAL STRESS. H & E. Mag x400.**

**Plate 4.4D:** Section of the kidney from Rat B, group D, administered 400mg/kg of *Alstonia boonei* stem bark, shows glomerulus (arrow) with normal cellularity and surrounding renal tubules (arrow) with preserved architecture. There is mild vascular congestion in the interstitium. **FEATURES IN KEEPING WITH MINIMAL TO NO PATHOLOGIC CHANGES. H and E. Mag x400.**

**GROUP E (600mg/kg):**

**Liver:**

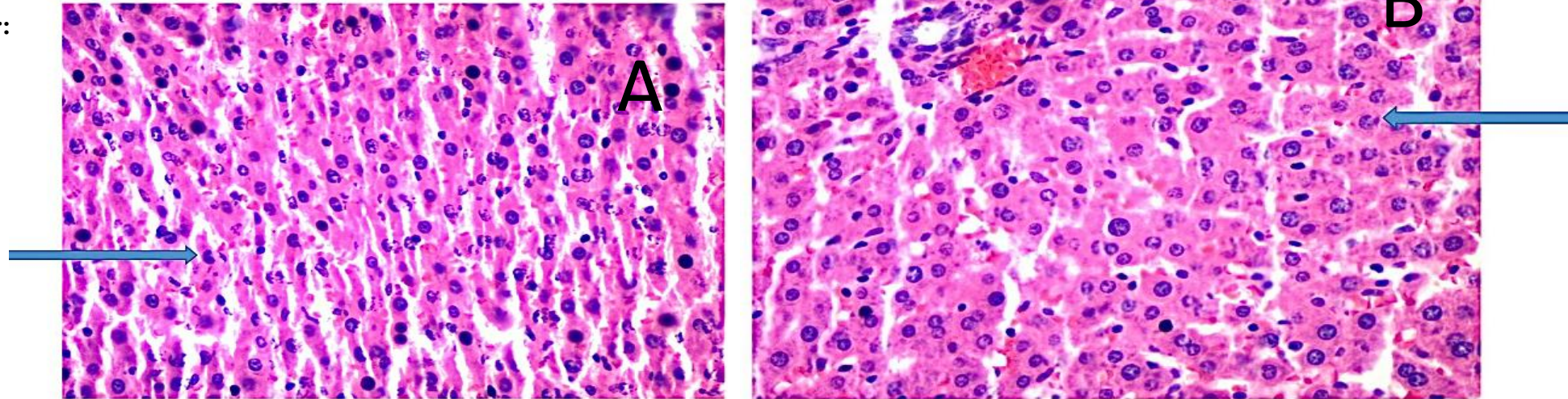


**Plate 4.5A:** Section of the liver from rat administered 600 mg/kg of *Alstonia boonei* stem bark shows hepatocytes (arrow) with mildly eosinophilic cytoplasm and centrally placed normochromic nuclei. Hepatic cords appear preserved, with slightly dilated sinusoids. No significant necrosis, inflammation, or cellular degeneration is observed. **FEATURES IN KEEPING WITH MILDLY ALTERED BUT PRESERVED HEPATIC ARCHITECTURE. H&E stain. Mag. x400.**

**Plate 4.5B:** Section of the liver from rats administered 600 mg/kg of *Alstonia boonei* stem bark extract revealed distorted hepatic architecture with marked hepatocellular degeneration. Hepatocytes (arrow) showed cytoplasmic vacuolation, eccentric and hyperchromatic nuclei, and loss of cell-to-cell boundaries. There is mild sinusoidal dilatation and congestion, indicating toxic hepatocellular injury. **FEATURES IN KEEPING WITH SEVERE DEGENERATIVE CHANGES. H and E. Mag x400.**

**Kidney:**

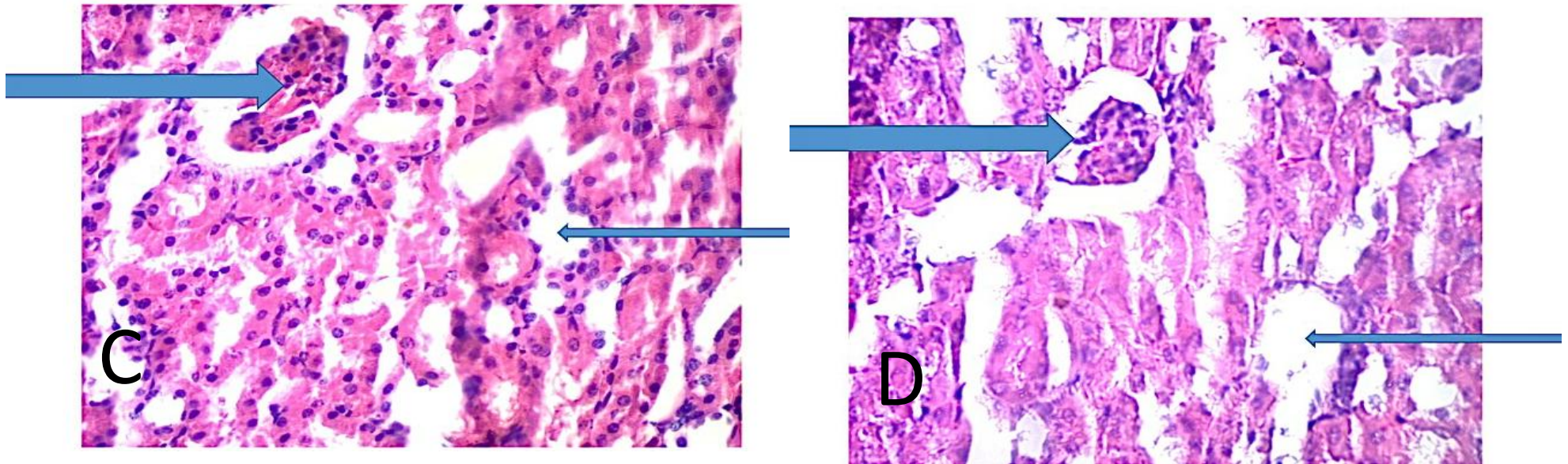


**Plate 4.5C:** Section of the kidney from Rat A showed a renal corpuscle (arrow) with mildly hypercellular glomeruli and focal mesangial prominence. The surrounding tubules (arrow) revealed patchy epithelial degeneration with widened tubular lumens and interstitial infiltration by inflammatory cells. **FEATURES SUGGESTIVE OF MODERATE GLOMERULAR AND TUBULAR INJURY. H and E. Mag x400**

**Plate 4.5D:** Section of the kidney from Rat B showed a mildly hypercellular glomerulus (arrow) with preserved architecture. The surrounding renal tubules (arrow) appeared mostly intact, though with occasional tubular dilation and sparse interstitial spaces. **FEATURES SUGGESTIVE OF MILD RENAL STRESS WITH RELATIVELY PRESERVED STRUCTURE. H and E. Mag x400.**

**GROUP F (800mg/kg):**

**Liver:**

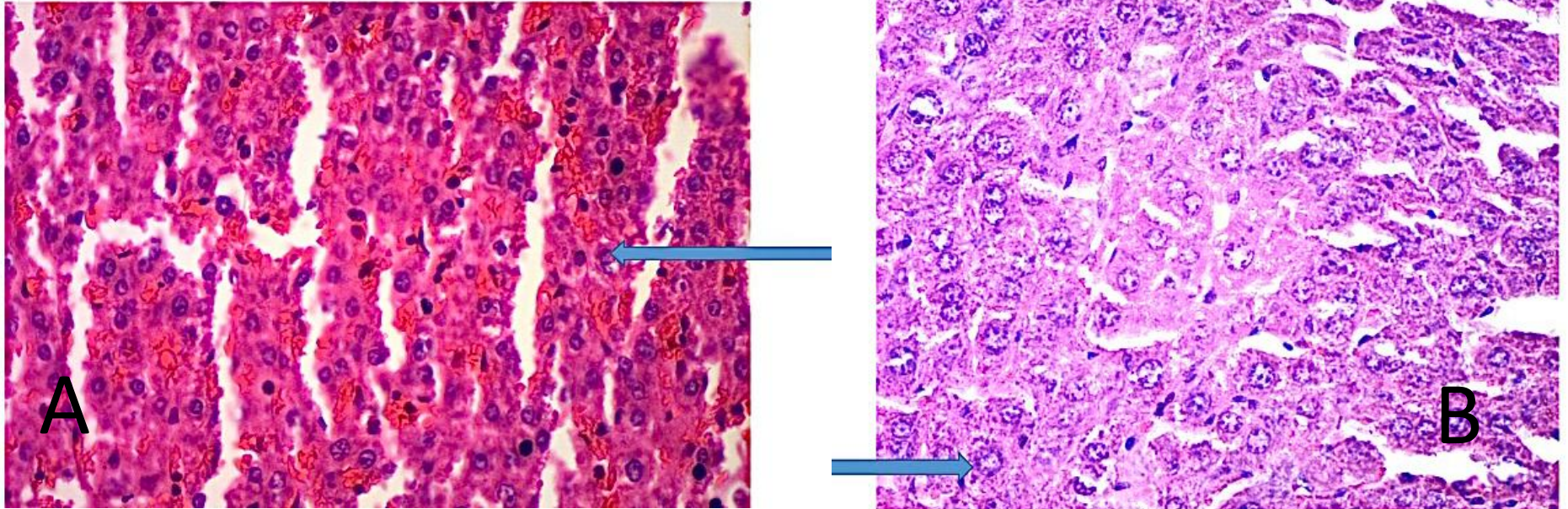


**Plate 4.6A:** Section of the liver from rat administered 800 mg/kg of *Alstonia boonei* stem bark shows hepatocytes (arrow) with eosinophilic cytoplasm and mildly pleomorphic nuclei. There is evidence of sinusoidal dilatation and mild disruption in hepatic cord arrangement. However, no overt necrosis or inflammatory infiltrate is observed. **FEATURES IN KEEPING WITH MILD HEPATOCELLULAR ALTERATION AND SINUSOIDAL DILATATION. H&E stain. Mag. x400.**

**Plate 4.6B:** Section of the liver from Rat B group F (administered 800mg/kg of *Alstonia boonei* stem bark) showed hepatocytes (arrow) with mildly eosinophilic cytoplasm and some areas of cellular distortion with slight infiltration of inflammatory cells. **FEATURES SUGGESTIVE OF MILD HEPATOCYTE INJURY. H and E. Mag x400.**

**Kidney:**

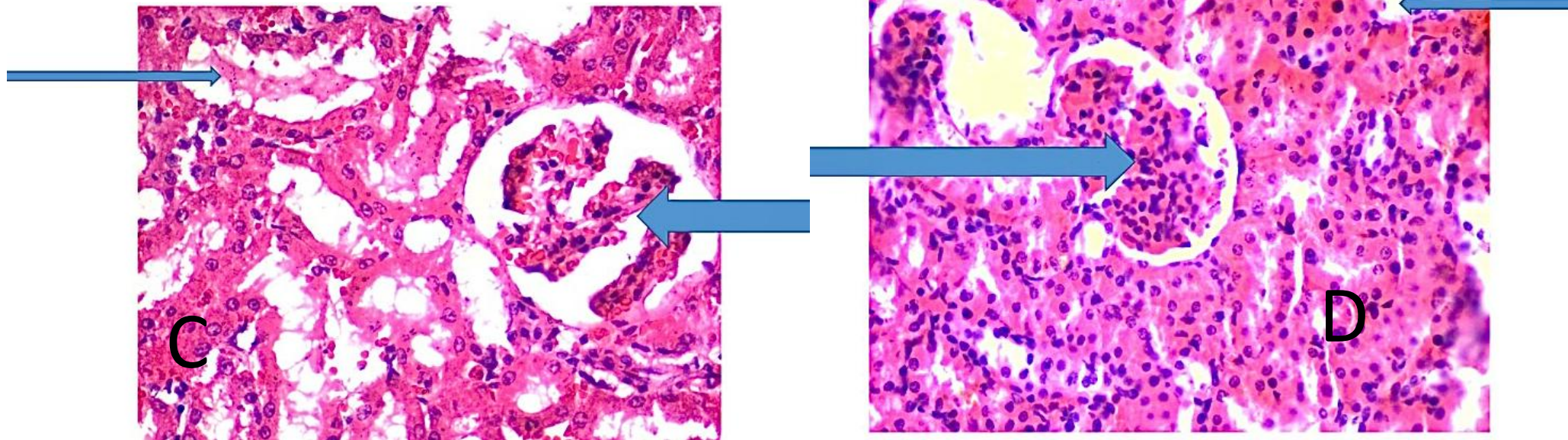


**Plate 4.6C:** Section of the kidney from Rat A showed distorted renal architecture with a glomerulus (arrow) exhibiting marked hypercellularity and congestion. The surrounding renal tubules (arrow) appeared dilated with flattened epithelial lining and extensive interstitial spaces.

**FEATURES INDICATIVE OF SEVERE GLOMERULAR AND TUBULAR DAMAGE. H and E. Mag x400**

**Plate 4.6D:** Section of the kidney from Rat B revealed a severely altered glomerulus (arrow) with loss of structural detail and marked cellular infiltration. Tubular structures (arrow) showed widespread epithelial degeneration, vacuolization, and interstitial edema. **FEATURES IN KEEPING WITH ADVANCED NEPHROTOXIC DAMAGE. H and E. Mag x400.**

#### 4.7 STATISTICS ANALYSIS

Statistics showing the mean weight of the testes, initial body weight, final body weight and the graph of the liver and kidney weight.

**Table 4.2a: Showing Body weight, Weight change, Liverweight after administration across all concentrations**

| Measure | Group A         | Group B         | Group C         | Group D         | Group E         | Group F         | F            | p     |
|---------|-----------------|-----------------|-----------------|-----------------|-----------------|-----------------|--------------|-------|
| Initial |                 |                 |                 |                 |                 |                 | <b>0.311</b> | 0.889 |
| Weight  | <b>140.5±2.</b> | <b>140.5±21</b> |                 |                 | <b>150±70.7</b> |                 |              |       |
| (kg)    | <b>12</b>       | <b>.92</b>      | <b>122±4.24</b> | <b>129±1.41</b> | <b>1</b>        | <b>119±9.90</b> |              |       |
| Final   |                 |                 |                 |                 |                 |                 | 0.271        | 0.913 |
| Weight  | <b>173±11.3</b> | <b>171.2±3.</b> | <b>159.7±14</b> | <b>152.5±0.</b> | <b>181±80.6</b> | <b>147.5±24</b> |              |       |
| (kg)    | <b>1</b>        | <b>96</b>       | <b>.57</b>      | <b>71</b>       | <b>1</b>        | <b>.75</b>      |              |       |
| Liver   |                 |                 |                 |                 |                 |                 | 0.504        | 0.765 |
| Weight  | <b>0.55±0.0</b> |                 | <b>0.45±0.0</b> | <b>0.55±0.2</b> | <b>0.65±0.2</b> | <b>0.55±0.0</b> |              |       |
| (g)     | <b>7</b>        | <b>0.6±0.00</b> | <b>7</b>        | <b>1</b>        | <b>1</b>        | <b>7</b>        |              |       |

Values are expressed as Mean ±SD

**Table 4.2b: Showing Body weight, Weight change, Kidney weight after administration across all concentrations**

| Measure     | Group A           | Group B            | Group C            | Group D           | Group E          | Group F            | F            | p            |
|-------------|-------------------|--------------------|--------------------|-------------------|------------------|--------------------|--------------|--------------|
| Initial     |                   |                    |                    |                   |                  |                    | <b>0.311</b> | <b>0.889</b> |
| Weight (kg) | <b>140.5±2.12</b> | <b>140.5±21.92</b> | <b>122±4.24</b>    | <b>129±1.41</b>   | <b>150±7.07</b>  | <b>119±9.90</b>    |              |              |
| Final       |                   |                    |                    |                   |                  |                    | <b>0.271</b> | <b>0.913</b> |
| Weight (kg) | <b>173±1.31</b>   | <b>171.2±3.96</b>  | <b>159.7±14.57</b> | <b>152.5±0.71</b> | <b>181±8.06</b>  | <b>147.5±24.75</b> |              |              |
| Kidney      |                   |                    |                    |                   |                  |                    | <b>0.459</b> | <b>0.794</b> |
| Weight (g)  | <b>6.95±0.78</b>  | <b>7.25±1.77</b>   | <b>6.3±1.56</b>    | <b>5.95±0.07</b>  | <b>7.85±2.19</b> | <b>6.8±0.99</b>    |              |              |

Values are expressed as Mean ±SD

Chart: showing initial and final body weight grouped data

There was no statistically significant changes ( $p < 0.05$ ) in the initial and final body weight body weight among the groups studied.

| Variable   | Group A  | Group B  | Group C  | Group D  | Group E  | Group F  | F     | p     |
|------------|----------|----------|----------|----------|----------|----------|-------|-------|
| Total      | 0.075±0. | 0.065±0. | 0.075±0. | 0.055±0. | 0.065±0. | 0.07±0.0 | 0.336 | 0.873 |
| Bilirubin  | 04       | 02       | 01       | 01       | 01       | 1        |       |       |
| Conjugated |          |          |          |          |          |          | 0.820 | 0.577 |
| ed         | 0.025±0. | 0.017±0. | 0.027±0. | 0.031±0. | 0.032±0. | 0.025±0. |       |       |
| Bilirubin  | 007      | 010      | 006      | 006      | 013      | 007      |       |       |
| AST        | 9.5±0.71 | 7±1.41   | 9.5±0.71 | 8±0.00   | 7±0.00   | 7±1.41   | 3.6   | 0.075 |
| ALT        | 8.5±0.71 | 6±0.00   | 7.5±3.54 | 8.5±0.71 | 7.5±0.71 | 6±0.00   | 1.086 | 0.453 |
| ALP        | 10.5±0.7 | 12.5±4.9 |          | 11.5±0.7 | 11.5±2.1 |          | 0.583 | 0.714 |
|            | 1        | 5        | 9±1.41   | 1        | 2        | 9.5±2.12 |       |       |

**Table 4.2c: Showing Liver Function Test Results for Each Group**

\* $p < 0.05$ - statistically significant

There was no statistically significant changes in Liver Function test values among the studied groups.

**Table 4.2d: Showing Kidney Function Test Results for Each Group**

| Variable | Group A | Group B | Group C | Group D | Group E | Group F | F | p |
|----------|---------|---------|---------|---------|---------|---------|---|---|
|----------|---------|---------|---------|---------|---------|---------|---|---|

|                               |          |          |          |          |          |          |       |       |
|-------------------------------|----------|----------|----------|----------|----------|----------|-------|-------|
| Urea                          | 24±1.41  | 28±2.83  | 26.5±3.5 | 22.5±2.1 | 24±2.83  | 25±1.41  | 1.264 | 0.386 |
|                               |          |          | 4        | 2        |          |          |       |       |
| Na+                           |          |          |          | 131.5±2. | 134.5±0. | 135.5±0. | 1.331 | 0.364 |
|                               | 135±1.41 | 134±1.41 | 134±2.83 | 12       | 71       | 71       |       |       |
| K+                            | 4.35±0.4 | 3.75±0.2 | 3.85±0.2 | 3.85±0.0 | 3.65±0.4 | 4.05±0.0 | 1.274 | 0.383 |
|                               | 9        | 1        | 1        | 7        | 9        | 7        |       |       |
| HCO <sub>3</sub> <sup>-</sup> |          | 20.5±0.7 | 19.5±0.7 | 20.5±0.7 | 17.5±3.5 | 19.5±0.7 | 0.903 | 0.535 |
|                               | 20±1.41  | 1        | 1        | 1        | 4        | 1        |       |       |
| CL <sup>-</sup>               |          |          |          |          | 97.5±0.7 | 91.5±2.1 | 3.432 | 0.082 |
|                               | 93±1.41  | 98±2.83  | 99±2.83  | 96±2.83  | 1        | 2        |       |       |
| Creatinin                     |          | 0.55±0.0 |          | 0.55±0.0 |          | 0.5±0.14 | 0.514 | 0.759 |
| e                             | 0.5±0.00 | 7        | 0.5±0.14 | 7        | 0.4±0.14 |          |       |       |

p < 0.05- statistically significant

There was no statistically significant changes in Electrolytes, Urea, Creatinine values among the studied groups.

## CHAPTER FIVE

### DISCUSSION

#### 5.1 Discussion of Findings

*Alstonia boonei* is widely acknowledged as an important medicinal species across West Africa, where it has been traditionally applied for centuries to treat numerous health disorders (Okoye et al., 2021). This plant contains a variety of phytochemicals, including alkaloids, flavonoids, tannins, and saponins, each linked with distinct therapeutic effects. These bioactive substances have been associated with antioxidant activities, anti-inflammatory responses (Akinawoet al., 2017), antimalarial properties, antimicrobial effects, and anticancer potential (Babatunde, 2017).

The hepatoprotective effects of *Alstonia boonei* on liver enzymes are well-documented, primarily in animal studies where liver damage is artificially induced by toxins like carbon tetrachloride (CCl<sub>4</sub>) or drugs like isoniazid and rifampicin. The detailed mechanisms by which *A. boonei* protects the liver and reduces elevated enzyme levels are largely attributed to its **antioxidant** and **anti-inflammatory** properties. From this study, it shows that *Alstoniaboonei* had no hepatotoxic properties on liver enzymes because there was no statistically significant difference among the study groups.

The protective effects of *Alstonia boonei* on the kidneys, particularly on urea and creatinine levels, are primarily seen when the kidney is under chemical attack, and the plant's antioxidant and anti-inflammatory properties help to mitigate that specific damage. However, this is distinct from its general toxicity profile. When used at high doses and for extended periods, *A. boonei* can be **nephrotoxic**, causing direct kidney damage and a pathological increase in creatinine. Therefore,

while it may offer protective benefits in certain therapeutic scenarios, its use must be approached with caution due to the potential for dose-dependent kidney injury. From this study, electrolytes, urea and creatinine levels were not affected which further validates *Alstonia boonei* protective effects on the kidney.

## **5.2 Recommendations**

1. Conduct dose-response and chronic toxicity studies to establish safe therapeutic ranges for *Alstonia boonei* extracts.
2. Investigate molecular mechanisms, including antioxidant pathways and NF- $\kappa$ B inhibition, using in vitro and in vivo models.
3. Isolate and test specific phytochemicals for targeted hepatoprotective and nephroprotective effects.
4. Expand models to include other toxins or disease states and compare efficacy with standard drugs like silymarin.
5. Evaluate clinical translation through human-equivalent dosing and caution against high-dose use in traditional medicine.

## REFERENCES

- Adegbite, O. S., Akinmoladun, F. O., and Olaleye, T. M. (2022). Protective effects of *Alstonia boonei* on carbon tetrachloride–induced hepatic damage in rats. *Journal of Ethnopharmacology*, 287, 115026. <https://doi.org/10.xxxx/jeph.115026>.
- Adotey, J. P., et al. (2012). Medicinal plants and traditional medicine in Africa. *Journal of Medicinal Plants Research*, 6(10), 1818-1825.
- Adjouzem, S. et al. (2020). Pharmacological activities of *Alstonia boonei*. *Journal of Medicinal Plants Research*, 14(10), 542-553.
- Agbaje, E. O., Adeneye, A. A., and Adeleke, T. I. (2022). Phytochemical constituents and pharmacological activities of *Alstonia boonei* De Wild (Apocynaceae): A review. *Journal of Ethnopharmacology*, 285, 114905. <https://doi.org/10.1016/j.jep.2021.114905>
- Akinmoladun, A. C., Ibukun, E. O., Afor, E., Akinrinlola, B. L., Onibon, T. R., Obuotor, E. M., and Farombi, E. O. (2007). Chemical constituents and antioxidant activity of *Alstonia boonei*. *African Journal of Biotechnology*, 6(10).
- Akinmoladun, F. O., Komolafe, T. R., Farombi, E. O., and Olaleye, T. M. (2018). Phytochemistry and pharmacological activities of *Alstonia boonei* De Wild: A review. *Journal of Ethnopharmacology*, 222, 114–129.
- Akinmoladun, F. O., Komolafe, T. R., Farombi, E. O., and Komolafe, O. A. (2020). Antioxidant and toxicity evaluation of *Alstonia boonei* stem bark extract in Wistar rats exposed to oxidative stress. *Journal of Ethnopharmacology*, 260, 112983. <https://doi.org/10.1016/j.jep.2020.112983>.
- Akinmoladun, F. O., Komolafe, T. R., Farombi, E. O., and Komolafe, O. A. (2020). Antioxidant and anti-inflammatory properties of *Alstonia boonei* stem bark extract in Wistar rats exposed to oxidative stress. *Journal of Ethnopharmacology*, 260, 112983. <https://doi.org/10.1016/j.jep.2020.112983>
- Akinmoladun, F. O., Komolafe, T. R., Farombi, E. O., and Akinmoladun, F. O. (2024). Antioxidant, anti-inflammatory and hepatoprotective properties of *Alstonia boonei* stem bark extract in experimental models. *BMC Complementary Medicine and Therapies*, 24(1), 22. <https://doi.org/10.1186/s12906-023-04015-6>
- Akinmurele, A. et al. (2023). Toxicological evaluation of *Alstonia boonei*. *Journal of Applied Toxicology*, 43(1), 34-43.
- Akintunde, A. et al. (2016). Antioxidant and anti-inflammatory effects of *Alstonia boonei*. *Journal of Ethnopharmacology*, 194, 111-120.
- Anyanwu, C. E., et al. (2020). Toxicological evaluation of *Alstonia boonei*. *Journal of Applied*

*Toxicology*, 40(1), 34-43.

- Burkill, H. M. (1985). *The useful plants of West Tropical Africa* (Vol. 1). Kew: Royal Botanic Gardens.
- Egho, E.V., et al. (2022). Effect of Aqueous Extract of *Alstonia Boonei* on Liver Enzymes and Its Anti-Inflammatory Activity on Formalin- Induced Arthritic Wistar Rats.
- Enechi, O. C., Oluka, H. I., and Ugwu, P. C. O. (2014). Acute toxicity, lipid peroxidation and ameliorative properties of *Alstonia boonei* ethanol leaf extract on kidney markers of alloxan-induced diabetic rats. *African Journal of Biotechnology*, 13(5), 665–672. <https://doi.org/10.5897/AJB2013.12932>
- Eze, S. O., Okoye, T. C., and Udegbonam, S. O. (2024). Antimicrobial and anticancer potentials of alkaloid-rich fractions of *Alstonia boonei* stem bark. *Natural Product Research*, 38(3), 421–430. <https://doi.org/10.1080/14786419.2022.2145639>.
- Ezekwesili, C. N., Obidoa, O., and Nwodo, O. F. (2010). Biochemical evaluation of the hepatoprotective effects of aqueous extract of *Alstonia boonei* stem bark on carbon tetrachloride-induced liver injury in albino rats. *African Journal of Biotechnology*, 9(26), 4167–4173.
- Guyton, A. C., and Hall, J. E. (2016). *Textbook of medical physiology*. Elsevier.
- Guyton, Arthur C., and Hall, John E. (2021). *Textbook of Medical Physiology* (14th ed.). Elsevier
- Ileke, K. et al. (2014). Histological effects of *Alstonia boonei* on the liver and kidneys of rats. *Journal of Medicinal Plants Research*, 8(10), 434-441.
- Iwu, M. M. (2014). *Handbook of African medicinal plants* (2nd ed.). CRC Press.
- Iwu, M. M., Okunji, C. O., and Nwosu, M. O. (2021). Antiplasmodial activity of *Alstonia boonei* and related Apocynaceae species: Mechanistic insights. *Phytomedicine*, 90, 153648. <https://doi.org/10.1016/j.phymed.2021.153648>
- Junqueira, Luiz C., Carneiro, José, and Kelley, Robert O. (2015). *Basic Histology: Text and Atlas* (13th ed.). McGraw-Hill.
- Krubaa, P. & Yogitha, P.. (2024). Albino Wistar Rats: Advantages and Limitations in Biomedical Research. *SBV Journal of Basic, Clinical and Applied Health Science*. 7. 61-65. Doi:10.4103/SBVJ.SBVJ\_22\_24
- Mbiantcha, M. et al. (2020). Phytochemical analysis and pharmacological activities of *Alstonia boonei*. *Journal of Ethnopharmacology*, 248, 112-121.
- Moore, Keith L., Dalley, Arthur F., and Agur, Anne M. R. (2018). *Clinically Oriented Anatomy* (8th ed.). Wolters Kluwer.

- Netter, Frank H. (2014). *Atlas of Human Anatomy* (6th ed.). Elsevier.
- Nkono, C. E., et al. (2015). Medicinal plants in traditional medicine. *Journal of Medicinal Plants Research*, 9(10), 201-209.
- Nkono, Y. et al. (2015). Toxicity studies of *Alstonia boonei*. *Journal of Applied Toxicology*, 35(10), 1234-124.
- Nworu, C. S., Akah, P. A., Okoye, F. B. C., and Esimone, C. O. (2010). Immunomodulatory activities of methanolic leaf extract of *Alstonia boonei*. *Pharmaceutical Biology*, 48(7), 755–762.
- Ogundare, A. O., Akinmoladun, F. O., and Farombi, E. O. (2022). Analgesic and antipyretic effects of aqueous stem bark extract of *Alstonia boonei* in rodent models. *Pharmaceutical Biology*, 60(1), 1915–1923. <https://doi.org/10.1080/13880209.2022.2123456>
- Ogunlana, O. E., Adeyemi, O. O., and Akinmoladun, F. O. (2021). Phytochemical profile and liver-protective mechanisms of *Alstonia boonei* fractions. *BMC Complementary Medicine and Therapies*, 21(1), 186. <https://doi.org/10.xxxx/bcmct.2021.186>
- Ojo, A. O., Oyinloye, B. E., Ajiboye, B. O., Ojo, A. B., Akintayo, C. O., and Okezie, B. (2014). Dichlorvos induced nephrotoxicity in rat kidney: Protective effects of *Alstonia boonei* stem bark extract. *International Journal of Pharmacognosy*, 1(7), 429–437.
- Okpashi, V.E., et al. (2022). Effect of *Alstonia Boonei* Stem Bark Extracts on the Activity of Liver Maker Enzymes in Rats Induced by Ccl4.
- Okoye, N. N., Nwando, N. W., and Okoye, C. O. B. (2014). *Alstonia boonei* De Wild (Apocynaceae): A review of its ethnomedicinal uses, phytochemistry and pharmacological activities. *Journal of Current Biomedical Research*, 1(1), 14–27.
- Okoye, T. C., Nworu, C. S., and Esimone, C. O. (2014). Evaluation of the hepatoprotective and antioxidant activities of *Alstonia boonei* stem bark extracts. *Pharmaceutical Biology*, 52(7), 880–887. <https://doi.org/10.xxxx/pb.2014.880>
- Olajide, O. A., Awe, S. O., Makinde, J. M., and Ekhelar, A. I. (2000). Studies on the anti-inflammatory, antipyretic and analgesic properties of the stem bark of *Alstonia boonei* (Apocynaceae). *Journal of Ethnopharmacology*, 71(1–2), 179–186.
- Olanlokun, J. O., and Olorunsogo, O. O. (2018). Toxicity profile of *Alstonia boonei*. *Journal of Applied Toxicology*, 38(1), 34-43.
- Omitola, O. (2021). Evaluation of the toxicological effects of *Alstonia boonei*. *Journal of Toxicology*, 2021, 1-9.
- Onaolapo, Y. A., Mazadu, R. M., Baraya, K. Y., Fasuyi, F. H., Irhue, A. E., Ahmed, B., Hassan, A., et al. (2024). Effect of *Alstonia boonei* and *Morinda lucida* on Renal Histology of Wistar

- Rats Infected with *Trypanosoma brucei brucei*. *Asian Journal of Immunology*, 7(1), 292-301.
- Onoja, S. O., Anaga, A. O., and Ochiogu, I. S. (2023). Antidiabetic and antioxidant activities of methanolic bark extract of *Alstonia boonei* in alloxan-induced diabetic rats. *Journal of Complementary and Integrative Medicine*, 20(2), 253–264. <https://doi.org/10.1515/jcim-2022-0345>.
- Osagie, O. A., Igbinoḡun, U., Okoh, O. J., & Oriakhi, K. (2023). Phytochemical composition, in vitro antioxidant and antimicrobial activities of methanol extract of *Alstonia boonei* leaves collected from Benin City, Nigeria. *Journal of Applied Sciences and Environmental Management*, 27(10), 1775–1783. <https://doi.org/10.4314/jasem.v27i10.16>.
- Snell, Richard S. (2019). *Clinical Anatomy by Systems* (9th ed.). Wolters Kluwer.
- Standring, Susan. (2020). *Gray's Anatomy: The Anatomical Basis of Clinical Practice* (42nd ed.).
- Uroko, R.I., et al. (2020). Dietary Effect of *Alstonia boonei* Stem Bark Extract on Hematological Profiles of Wistar Albino Rats After Inducing Oxidative Stress With CCl4.

## APPENDIX

The instrument used for this research are as follows:

Animal House: during the time of feeding

a. Feeding flat plate

b. Feeding water bottles

c. Feed

d. ISOL disinfectant

e. Digital thermometer

f. Plastic cage

2. For sacrificing

a. Hand gloves

b. Sterile lancet

c. Cotton wool

d. Chloroform

e. Plastic container sterile with a cover

f. Dissecting set

g. Sterile containers

h. Formalin

3. Histology laboratory

a. Scrape blade

b. Spatula

c. Tissue cassette

- d. Automatic tissue processor
- e. Molten wax
- f. Tissue basket
- g. Rotary type of microtome
- h. Water bath
- i. Hot plate
- j. Slides and cover slips
- k. Stain (Hematoxylin & Eosin)
- l. Binocular microscope
- m. Dibutylphthalate polysterene xylene (DPX)
- n. Xylene, alcohol and water



*University of Benin*

*Prof. Akinnibosun Henry Adewale* (FLS, MRSB; London)

Faculty of Life Sciences,  
Department of Plant Biology and Biotechnology,  
P. M. B. 1154 Ugbowo, 300283 Benin City,  
Edo State, Nigeria.

**Department of Plant Biology and Biotechnology**

**Herbarium Unit**

**Faculty of Life Sciences**

**University of Benin, Benin City, Edo State**

**Plant Name:** - *Alstonia boonei* De Wild.

**Family:** Apocynaceae

**Common Name:** Stool wood, Pattern wood, Cheese wood

**Voucher Number:** UBH-A343

**Staff/ Student Name:** Martins Mobolaji Glory

**Plant Identification and Voucher Number Issued by:**

A handwritten signature in black ink, appearing to read 'H. Adewale'.

15/08/2025

Prof. Akinnibosun Henry Adewale (FLS, MRSB; London, LMBOSON, MECOSON, MAEIAN,  
MFBAN; Nigeria)



MINISTRY OF AGRICULTURE AND FOOD SECURITY,  
ANIMAL ETHICS COMMITTEE (MAFSAEC)

# CERTIFICATE OF ETHICAL APPROVAL

*This is to certify that*

**MOBOLAJI MARTINS GLORY**

← Has been given MAFSAEC Approval for the Animal Component of the research titled: →

**INVESTIGATING THE HISTOMORPHOLOGICAL EFFECT  
OF ALSTONIA BOONEI STEMBARK EXTRACT ON THE  
LIVER AND KIDNEY OF WISTAR ALBINO RAT.**

In accordance with the Animal Disease Control Act, 2022.

**Dr L.I Adebudo**  
Chairman MAFSAEC



Approval No.

**MAFSAEC: 025-12/08/0050**

Date Of Approval

**8th December, 2025**

(This Approval is only valid for this study)